

Are Trends in Convective Parameters over the United States and Europe Consistent between Reanalyses and Observations?

NATALIA PILGUJ,^a MATEUSZ TASZAREK,^{b,c,d} JOHN T. ALLEN,^c AND KIMBERLY A. HOOGEWIND^{c,d}

^a Faculty of Earth Sciences and Environmental Management, University of Wrocław, Wrocław, Poland

^b Department of Meteorology and Climatology, Adam Mickiewicz University, Poznań, Poland

^c Cooperative Institute for Severe and High-Impact Weather Research and Operations, University of Oklahoma, Norman, Oklahoma

^d NOAA/OAR/National Severe Storms Laboratory, Norman, Oklahoma

^e Central Michigan University, Mount Pleasant, Michigan

(Manuscript received 12 February 2021, in final form 3 January 2022)

ABSTRACT: In this work, long-term trends in convective parameters are compared between ERA5, MERRA-2, and observed rawinsonde profiles over Europe and the United States including surrounding areas. A 39-yr record (1980–2018) with 2.07 million quality-controlled measurements from 84 stations at 0000 and 1200 UTC is used for the comparison, along with collocated reanalysis profiles. Overall, reanalyses provide signals that are similar to observations, but ERA5 features lower biases. Over Europe, agreement in the trend signal between rawinsondes and the reanalyses is better, particularly with respect to instability (lifted index), low-level moisture (mixing ratio), and 0–3-km lapse rates as compared with mixed trends in the United States. However, consistent signals for all three datasets and both domains are found for robust increases in convective inhibition (CIN), downdraft CAPE (DCAPE), and decreases in mean 0–4-km relative humidity. Despite differing trends between continents, the reanalyses capture well changes in 0–6-km wind shear and 1–3-km mean wind with modest increases in the United States and decreases in Europe. However, these changes are mostly insignificant. All datasets indicate consistent warming of almost the entire tropospheric profile, which over Europe is the fastest near ground whereas across the Great Plains it is generally between 2 and 3 km above ground level, thus contributing to increases in CIN. Results of this work show the importance of intercomparing trends between various datasets, as the limitations associated with one reanalysis or observations may lead to uncertainties and lower our confidence in how parameters are changing over time.


KEYWORDS: Europe; North America; Severe storms; Storm environments; Thunderstorms; Climatology; Convective storms; Storm environments; Radiosonde/rawinsonde observations; Reanalysis data; Trends

1. Introduction

Historical trends in severe thunderstorms are an important topic in the context of growing impacts of hazards and losses to the insurance industry (Sander et al. 2013; Brown et al. 2015; Munich Re 2020). However, it is still unclear how an anthropogenically warming climate is influencing these extreme events (Diftenbaugh et al. 2007, 2013; Gensini and Mote 2015; Trapp and Hoogewind 2016; Allen 2018; Rädler et al. 2019). A number of studies have explored the presence of historical trends using both direct observations (Verbout et al. 2006; Mohr and Kunz 2013; Allen and Tippett 2015; Tippett et al. 2016) and environments favorable to the development of convective storms derived from reanalyses (Robinson et al. 2013; Mohr et al. 2015; Gensini and Brooks 2018; Rädler et al. 2018; Tang et al. 2019; Taszarek et al. 2021a; Lepore et al. 2021). Detecting trends in convective hazards is not trivial, as observations are incomplete and vary in quality over time and space, over both the United States and Europe (Doswell et al. 2005; Verbout et al. 2006; Allen and Tippett 2015; Tippett et al. 2015;

Groenemeijer et al. 2017; Edwards et al. 2018; Taszarek et al. 2020a; Zhou et al. 2021).

The use of environmental proxies instead of direct observations provides the advantage of a more complete temporal and spatial record, but with limited confidence about whether convection initiates (Bunkers et al. 2010; Hoogewind et al. 2017; Romps et al. 2018; Tippett et al. 2019). Reanalyses also tend to struggle with appropriate sampling of thermodynamic instability and low-level wind shear, especially when considering extreme environments and sharp boundaries such as coastal zones and mountains (Thompson et al. 2003; Allen and Karoly 2014; Gensini et al. 2014; Taszarek et al. 2018; King and Kennedy 2019; Li et al. 2020; Taszarek et al. 2021b; Varga and Breuer 2021). Analysis of trends in different reanalysis datasets has also suggested that results can vary markedly (Robinson et al. 2013; Tang et al. 2019; Koch et al. 2021; Taszarek et al. 2021a), as most of these datasets are typically not designed or validated for this use, despite widespread application (Thorne and Vose 2010). While these studies have explored historical trends owing to differences in parameter calculations and methods, no study has explored how these trends in convective environments compare between reanalyses, nor whether these signals are consistent with observed soundings. However, homogenization of long-term radiosonde temperature data on a global scale has shown that even

 Denotes content that is immediately available upon publication as open access.

Corresponding author: Mateusz Taszarek, mateusz.taszarek@noaa.gov

DOI: 10.1175/JCLI-D-21-0135.1

© 2022 American Meteorological Society. For information regarding reuse of this content and general copyright information, consult the AMS Copyright Policy (www.ametsoc.org/PUBSReuseLicenses).

observations feature issues in temporal continuity (Zhou et al. 2021).

Environmental parameters favorable to the development of severe thunderstorms in many studies have been examined using proximity soundings from rawinsonde launches at nearby sites (Rasmussen and Blanchard 1998; Thompson et al. 2003; Potvin et al. 2010; Coniglio and Parker 2020). Atmospheric soundings reflect the true state of the atmosphere at a fixed point in time; however, they are disadvantaged by the frequency of sampling and by the spatial distribution of release sites, which correspond with populated areas. Typical sampling is twice daily at 0000 and 1200 UTC by convention, and is not necessarily well timed with the diurnal peak in convective parameters and frequency of severe thunderstorms (Groenemeijer and Kühne 2014; Krocak and Brooks 2018; Taszarek et al. 2020a,b). Soundings are also subject to failures in sampling, such as instrument malfunction, adverse weather, or poor vertical resolution, which can render a sampled profile unusable. This suggests that leveraging sounding datasets for long temporal periods requires careful quality control of profiles, and selection of sites with long continuous records on which to perform such an analysis.

Reanalysis by contrast provides uniform sampling of the environment corresponding to model analysis timing, a longer temporal record, and a uniform spatial grid of the underlying data. Evaluation of reanalysis products against observed soundings has suggested that they can reliably represent certain features of the atmospheric state related to convective environments, although performance varies from reanalysis to reanalysis (Allen and Karoly 2014; Gensini et al. 2014; Taszarek et al. 2018; King and Kennedy 2019). The reliability of reanalysis profiles of wind, temperature, and moisture has also been a focus of many prior studies (Graham et al. 2019; Alghamdi 2020; Hallgren et al. 2020; Han et al. 2021; Huang et al. 2021; Virman et al. 2021). Recent evaluations of ERA5 (Hersbach et al. 2020) and MERRA-2 (Gelaro et al. 2017) have shown that both produce correlations with soundings of ~ 0.8 for thermodynamic-related parameters and ~ 0.9 for wind-related parameters, with low mean errors (Taszarek et al. 2021b). However, ERA5 outperforms MERRA-2, in part as a result of the enhanced resolution that allows it to better represent the boundary layer (Varga and Breuer 2021). A number of limitations in reanalyses relate to their generation by model products that due to horizontal resolution must include convective parameterizations, which lead to disturbances of the diurnal cycle, underestimated instability, contamination of convective profiles or other unrealistic attributes (Allen et al. 2014; Tippet et al. 2014; King and Kennedy 2019). Despite this, as we show in this study, relatively consistent performance through time suggests that reanalyses are comparable to soundings for evaluation of long-term trends, despite the limitations associated with the changing volume of observations and other data that is assimilated.

Recent analyses using historical data have suggested that instability is increasing over Europe (Rädler et al. 2018; Taszarek et al. 2021a); however, the sign of the trend can vary over the United States depending on the reanalysis used (Gensini and Brooks 2018; Tang et al. 2019; Taszarek et al.

2021a), driven mainly by the uncertainty in changes of boundary layer moisture. Increases in storm-relative helicity has also been observed and linked to strengthening of the low-level jet over the Great Plains (Barandiaran et al. 2013; Tang et al. 2019). In contrast, changes to vertical wind shear have been modest and generally nonsignificant. Combinations of the aforementioned instability and shear parameters have suggested that increases to convective environments favorable to severe thunderstorms are likely (Gensini and Brooks 2018; Rädler et al. 2018; Tang et al. 2019; Lepore et al. 2021). However, recent findings from ERA5 heavily temper these results, as decreases to relative humidity and rapidly strengthening convective inhibition (CIN) lead to less efficient convective initiation and lower frequency of thunderstorms as a result (Taszarek et al. 2021a). This suggests that any future changes in the response to increasing instability or vertical wind shear may not necessarily lead to more frequent convective hazards, as changes to the frequency of initiation are uncertain. As this result has significant implications for thunderstorm occurrence, it raises the question of whether the ERA5 reliably indicates changes to convective environments through time. Two distinct possibilities are that the depicted changes are a reflection of the reanalysis formulation and temporal biases, or alternatively a signal found more broadly in observed soundings and other reanalysis products. By comparing a large sample of sounding profiles with ERA5, Taszarek et al. (2021b) suggested that ERA5 is likely one of the most reliable available reanalyses for exploration of convective environments, but its credibility in sampling long-term trends has not yet been evaluated. Therefore, building on the analysis of Taszarek et al. (2021a,b) and using these data, in this work we compare long-term trends in convective parameters and vertical profiles between rawinsonde measurements and ERA5 and MERRA-2 reanalyses over both Europe and the United States and their surrounding areas. Convective parameters are consistently calculated across the three datasets and assessed to ascertain whether these trends are reliable, robust, and meaningful through a variety of convectively important parameters. Signals consistent with all three datasets allow us to better assess the credibility of historical trends with respect to future changes, while those signals that notably differ allow us to highlight reanalysis-related issues that should be considered with caution.

2. Dataset and method

a. Sounding data

Observational data used in this study were derived from the atmospheric sounding database of the University of Wyoming (<http://weather.uwyo.edu/upperair/>). Here we evaluate all available upper-air observations for 0000 and 1200 UTC over the period 1980–2018 for 84 stations located across Europe and the United States including surrounding areas (Fig. 1a). Although not all evaluated sounding sites are located within the European and United States borders, we will use these terms in describing domains in this study for simplicity. Initially, soundings were downloaded from 232 stations [as in Taszarek et al. (2021b)], but in this study we chose

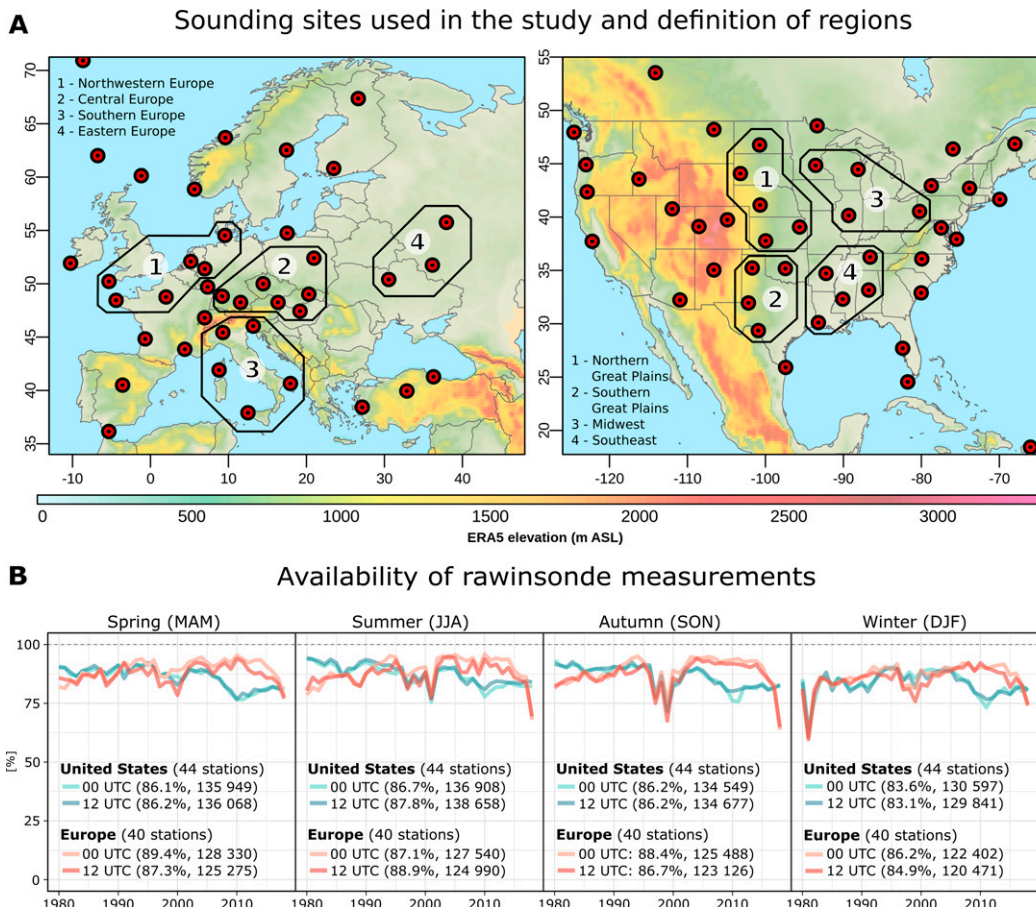


FIG. 1. (a) Sounding stations used in the analysis and definition of regions, and (b) mean number of 0000 and 1200 UTC observations over the seasons.

only those sites that ensured sufficient quality and continuity of measurements over the period of interest to allow credible trend computation. Using quality-control functions (detailed in the following paragraph) aimed at detecting obvious errors in vertical profiles of temperature, moisture, and wind, we removed poor-quality soundings that allowed us to choose final sites for the trend evaluation.

Profiles were discarded where the first measurement was higher than 10 m above ground level (AGL) and the highest level was lower than 6000 m AGL (to ensure correct calculation of vertical wind shear). Observations with fewer than 10 levels over the depth of the sounding were also excluded. It was required that each considered level have u and v wind components, temperature, moisture, height, and pressure data available. If any variable was missing, such levels were not considered. Only missing moisture observations higher than 6000 m AGL were acceptable as that was often the case for soundings from the 1980s and 1990s and was not necessary for calculation of metrics considered in this study. Soundings with unrealistic vertical changes of air temperature, moisture, or wind conditions were also removed. Temperature gradients between any pair of levels exceeding 12 K km^{-1} in the 0–2-km AGL layer and 10 K km^{-1} above 2 km AGL resulted in those

soundings also being removed. We also did not consider non-physical levels where air was saturated and dry-adiabatic at the same time. Mean dewpoint depression lower than 2°C for the entire profile also resulted in sounding removal. Quality control also extended to correction of the lowest 500 m AGL, where gradients of temperature exceeding 12 K km^{-1} were changed to 12 K km^{-1} by adjusting values of air temperature (to reduce any potential negative effect on the parcel calculations). Using selected temperature, wind, and moisture parameters, soundings that had values higher than the 0.99999th and lower than 0.00001th percentiles (considering the whole dataset) were removed.

Even though the applied quality-control techniques may remove a small fraction of good-quality profiles, they notably increase the overall quality of the sounding dataset. After quality control, we considered only those stations that contained at least 20 000 observations (512 per year) and a ratio between 0000 and 1200 UTC measurements ranging from 0.85 to 1.15 (to avoid thermodynamic biases resulting from higher number of profiles during day or night). This filter was aimed at focusing only on locations where trends were unlikely to be impacted by other factors. Nevertheless, the mean number of soundings per station was still usually slightly

TABLE 1. Parameters evaluated in the study.

Abbreviation	Full name	Units
MIXR	0–500-m mixed-layer mixing ratio	g kg^{-1}
CIN	0–500-m mixed-layer convective inhibition	J kg^{-1}
LI	0–500-m mixed-layer lifted index at 500 hPa	K
DCAPE	0–4000-m lowest theta-e downdraft convective available potential energy	J kg^{-1}
LR03	0–3000-m temperature lapse rate	K km^{-1}
BS06	0–6000-m bulk wind difference (wind shear)	m s^{-1}
BS01	0–1000-m bulk wind difference (wind shear)	m s^{-1}
RH04	0–4000-m mean relative humidity	%
MW13	1000–3000-m mean wind	m s^{-1}

higher for observations from 0000 UTC, which should be taken into account when comparing results with climatological records from ERA5 and MERRA-2 (Fig. 1b). In total, 2.07 million atmospheric soundings were obtained following filtering for use in this analysis, including ~1 million from 40 stations in the European domain, and another million from 44 stations situated in the United States domain. The number of available profiles was comparable among seasons, and the missing data accounted for around 15% of the total record equally distributed throughout the year (Fig. 1b).

Despite applied quality-control techniques, we note that there are a number of possible data inhomogeneities that may be caused by the relocation of sounding stations, instrument changes, or measurement practices. Because of that, the assumption that rawinsondes provide real long-term trends may be misleading. However, it has been a common practice in recent studies to consider rawinsonde observations as the reference to reanalysis evaluation (Bao and Zhang 2019; King and Kennedy 2019; Li et al. 2020; Varga and Breuer 2021; Wang et al. 2021).

b. Reanalyses and evaluated variables

ERA5 is the fifth-generation atmospheric reanalysis produced by ECMWF (Hersbach et al. 2020) available through the Copernicus Climate Change Service (2017). It has a regular latitude–longitude grid at $0.25^\circ \times 0.25^\circ$ resolution and 137 hybrid-sigma model levels up to 0.01 hPa. The density of levels in the lower troposphere (e.g., 28 levels in the layer of 0–2 km AGL) allows for detailed representation of conditions in the lower atmosphere that are crucial for thermodynamic metrics such as convective inhibition. ERA5 reanalysis is based around a 4D-Var assimilation method and provides hourly data with 12-h assimilation windows (at 0900 and 2100 UTC).

The second reanalysis is the Modern-Era Retrospective analysis for Research and Applications version 2 (MERRA-2; Gelaro et al. 2017) developed by NASA’s Global Modeling and Assimilation Office and based on a period of regular conventional and satellite observations starting in the 1980s. MERRA-2 has a $0.5^\circ \times 0.625^\circ$ horizontal grid spacing with 72 hybrid-sigma model levels; in contrast to ERA5, only 14 are included in the layer 0–2 km AGL. The reanalysis relies on a 3D-Var algorithm for assimilation based on the grid point statistical interpolation (GSI) with 6-h update cycle and

the “first guess at appropriate time” (FGAT) procedure and a temporal resolution of 3 h (Gelaro et al. 2017).

Both reanalyses were obtained for a period equivalent to the sounding data to match the nearest proximal grid to the selected sounding sites across Europe and the United States for all 0000 and 1200 UTC steps (Fig. 1a). As reanalyses do not suffer from the same quality control issues as observations, we used complete datasets for the profiles, while for soundings only the number of available measurements were used. Vertical profiles of temperature, humidity, height, pressure, and u and v wind components in all three datasets were processed with the R language package *thunder* (Taszarek et al. 2021b). To match surface conditions between soundings, ERA5 and MERRA-2, an interpolated level of 10 m AGL was chosen as a starting point for computations in all three datasets. Parameters evaluated in this study (Table 1) were chosen based on prior studies focusing on various aspects of severe convective storms across Europe and the United States (Craven and Brooks 2004; Gensini and Ashley 2011; Mohr and Kunz 2013; King and Kennedy 2019; Rädler et al. 2019; Chen et al. 2020; Liu et al. 2020; Taszarek et al. 2020b, 2021b). For calculation of the mixing ratio (MIXR), lifted index (LI), and CIN a mixed layer (ML) of 0–500 m AGL was used. Following Púčík et al. (2017), we use LI instead of CAPE as it is a continuous quantifier even if the atmosphere is stable whereas CAPE by its nature only represents buoyant atmosphere. Bulk wind shear parameters were computed as a magnitude between surface (10 m AGL) and heights of 1 km AGL (BS01) and 6 km AGL (BS06). Downdraft CAPE (DCAPE; Gilmore and Wicker 1998) was computed by calculating the lowest θ (theta-e) value in the layer of 0–4 km AGL and descended moist adiabatically to the surface. In this study we also present trends in a vertical profile of temperature interpolated every 100 m relative to the height above ground level. We do not evaluate trends in vertical profiles of dewpoint temperature, due to frequent gaps in rawinsondes data before 1990 and reliability of moisture measurements, especially in higher parts of the troposphere.

One of the most significant limitations of using reanalysis when compared with observed profiles is the horizontal grid spacing ($0.25^\circ \times 0.25^\circ$ for ERA5 and $0.5^\circ \times 0.625^\circ$ for MERRA-2), which results in vertical profiles reflecting an average over that grid at any individual level. Thus, reanalyses struggle with representation of local processes, most commonly seen along sharp boundaries such as mountains or

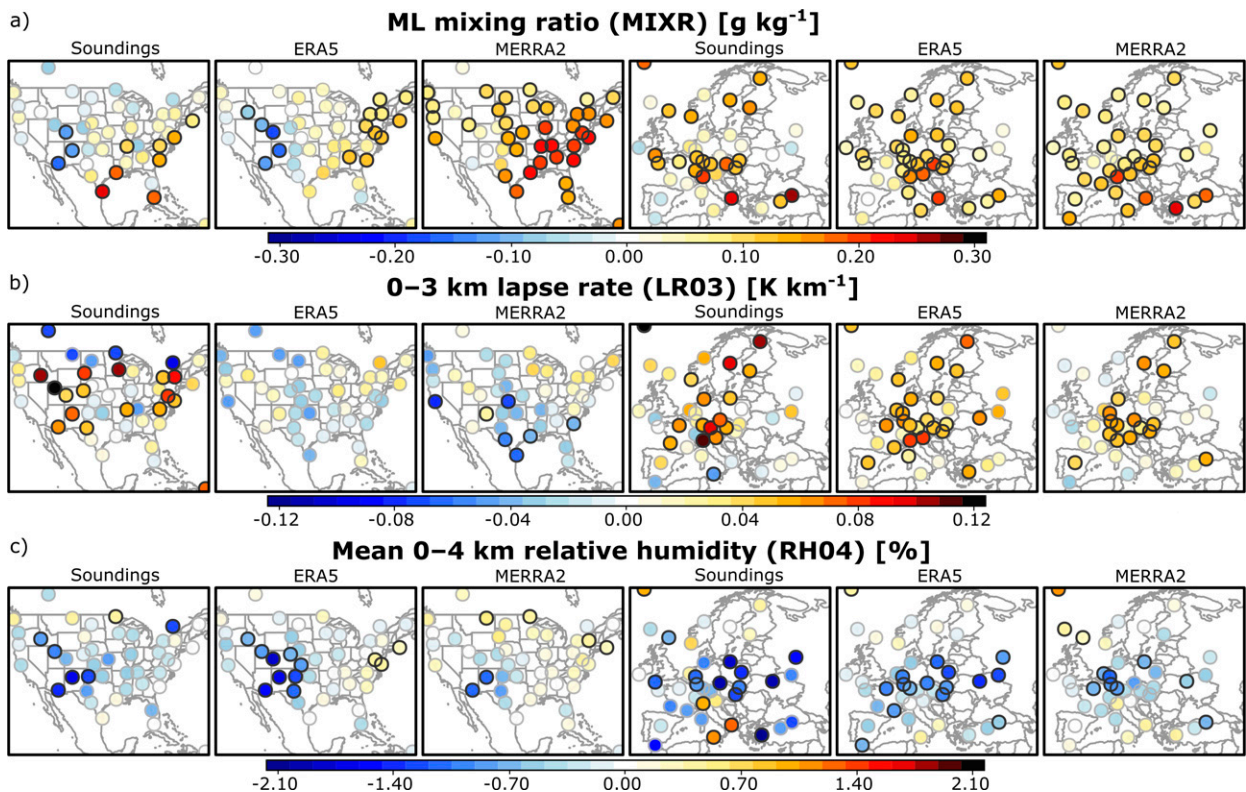


FIG. 2. Long-term trend per decade for (a) ML mixing ratio, (b) 0–3-km lapse rate, and (c) mean 0–4-km relative humidity, based on soundings, ERA5, and MERRA-2. Trend is derived from Sen's slope estimator. Black circles around each point denote p values below 0.05. Only 0000 and 1200 UTC time steps are considered.

coastal zones. Convective parameterization schemes applied in ERA5 and MERRA-2 can also lead to errors in the vertical profile of temperature and moisture as compared with rawinsonde observations (Allen et al. 2014; King and Kennedy 2019; Taszarek et al. 2021b; Varga and Breuer 2021; Wang et al. 2021). However, in this study these issues are of lower importance, as we focus on the magnitude and sign of the temporal change and any single-profile differences are reduced by the large sample size and climatological averaging. Although local biases with respect to absolute values of specific variables are still possible, we expect a slope of the trends to be consistent between all three datasets if the signal is credible and physically based.

c. Regionalization and trend computation

Long-term changes in selected convective parameters are considered for individual stations across Europe (40) and the United States (44; Fig. 1a). Based on annual means, trends are calculated for each dataset using the nonparametric Sen's slope estimator (Wilcox 2010). This method of trend calculation is nonparametric and more robust to outliers; thanks to these properties, it is commonly applied in atmospheric sciences, especially extreme events (e.g., Gensini and Brooks 2018; Tang et al. 2019; Masroor et al. 2020). In this research, a nonparametric Mann–Kendall two-tailed test and Sen's slope estimator was used to ascertain significant trends, at the $\alpha = 0.05$

level. Resulting trends are normalized to show changes per decade to improve interpretation. Calculations were provided using the R package *trend* (Sen 1968; Hipel and McLeod 1994).

In addition to individual station analysis, a regional aggregation of data was also considered, allowing us to minimize negative aspects arising from analysis of single-station data. For Europe this focused on the northwest, central, southeast, and eastern regions, and for the United States on the northern Great Plains, southern Great Plains, Midwest, and southeastern regions (as defined in Fig. 1a). Each region was chosen to consist of 3–7 stations. The slope of the trend was also computed for the mean values across the meteorological seasons March–May (MAM), June–August (JJA), September–November (SON), and December–February (DJF).

3. Results

a. Moisture and lapse rate parameters

Trends in near-surface moisture represented by observations indicate decreases over the western United States and significant increases over the eastern part of the country (Figs. 2 and 3). Results from ERA5 are in agreement with observations, but MERRA-2 provides increases over the entire United States, primarily during spring and summer (Fig. 3). The discrepancy in trends of MIXR between MERRA-

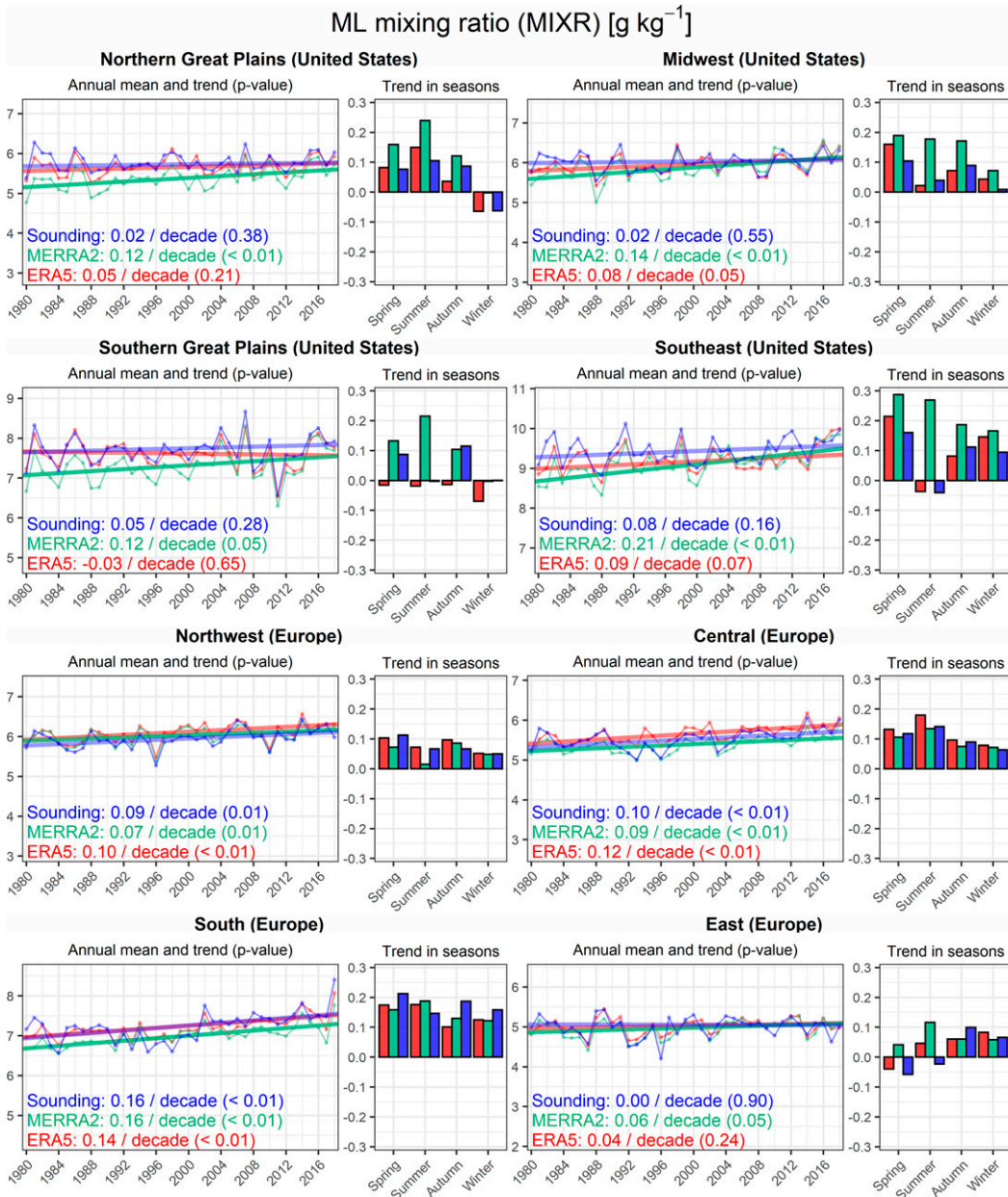


FIG. 3. Annual mean and corresponding long-term trend for the period 1980–2019 among European and U.S. regions for ML mixing ratio (blue for soundings, green for MERRA-2, and red for ERA5). Trend is derived from Sen's slope; values in the parentheses denote p value. Bars indicate trend values per decade over seasons. Only 0000 and 1200 UTC time steps are considered.

2 and observations is surprising, as this variable is generally well represented by MERRA-2 with high correlations and small mean errors (Taszarek et al. 2021b). This suggests that the primary source of error in MERRA-2 for the United States is most likely related to the quantity and quality of assimilated data over time (McCarty et al. 2016).

Across Europe, changes in low-level moisture are in much better agreement between the three datasets, with significant positive trends over the entire continent except the southwest

and east. The largest trends exceed $+0.2 \text{ g kg}^{-1}$ per decade and are observed for stations located in central and southern Europe (Fig. 2a). Seasonally, all datasets are consistent with increases of around $+0.1 \text{ g kg}^{-1}$ per decade, except spring and summer in eastern Europe where small insignificant decreases are indicated by soundings and ERA5 (Fig. 3). Considering absolute differences between reanalyses and soundings, MIXR is typically underestimated by reanalyses across the United States through time, whereas it is slightly overestimated for Europe (Fig. 3).



FIG. 4. As in Fig. 3, but for 0–3-km lapse rate.

For 0–3-km AGL lapse rates (LR03), mostly positive tendencies are observed for sounding sites across the United States, but in contrast the reanalyses show downward and insignificant trends (Fig. 2b). Lapse rates trends notably vary in space, especially over areas with complex terrain, which was also demonstrated for other parts of the world by Minder et al. (2010) and Kattel et al. (2012). A disparity in trends of LR03 is also observed among seasons. During spring and summer decreasing trends are observed across the northern Great Plains while increases occur during winter (Fig. 4). In the Midwest, there is a good agreement in terms of increases between reanalyses and soundings during summer, autumn,

and winter. The southern Great Plains and southeastern United States feature mixed trends.

In Europe, similar to MIXR, reanalyses and observations are in agreement and indicate significant increases to LR03 of around $+0.06 \text{ K km}^{-1}$ per decade across almost the entire continent except the Mediterranean area (Fig. 2b). The best agreement is found in central Europe where significant increases in LR03 occur all year round (Fig. 4). Over northwestern and southern Europe there are similar patterns, with the exception of spring where only modest changes take place (Fig. 4). For eastern Europe, the trend is inconsistent among the datasets during autumn and winter where MERRA-2

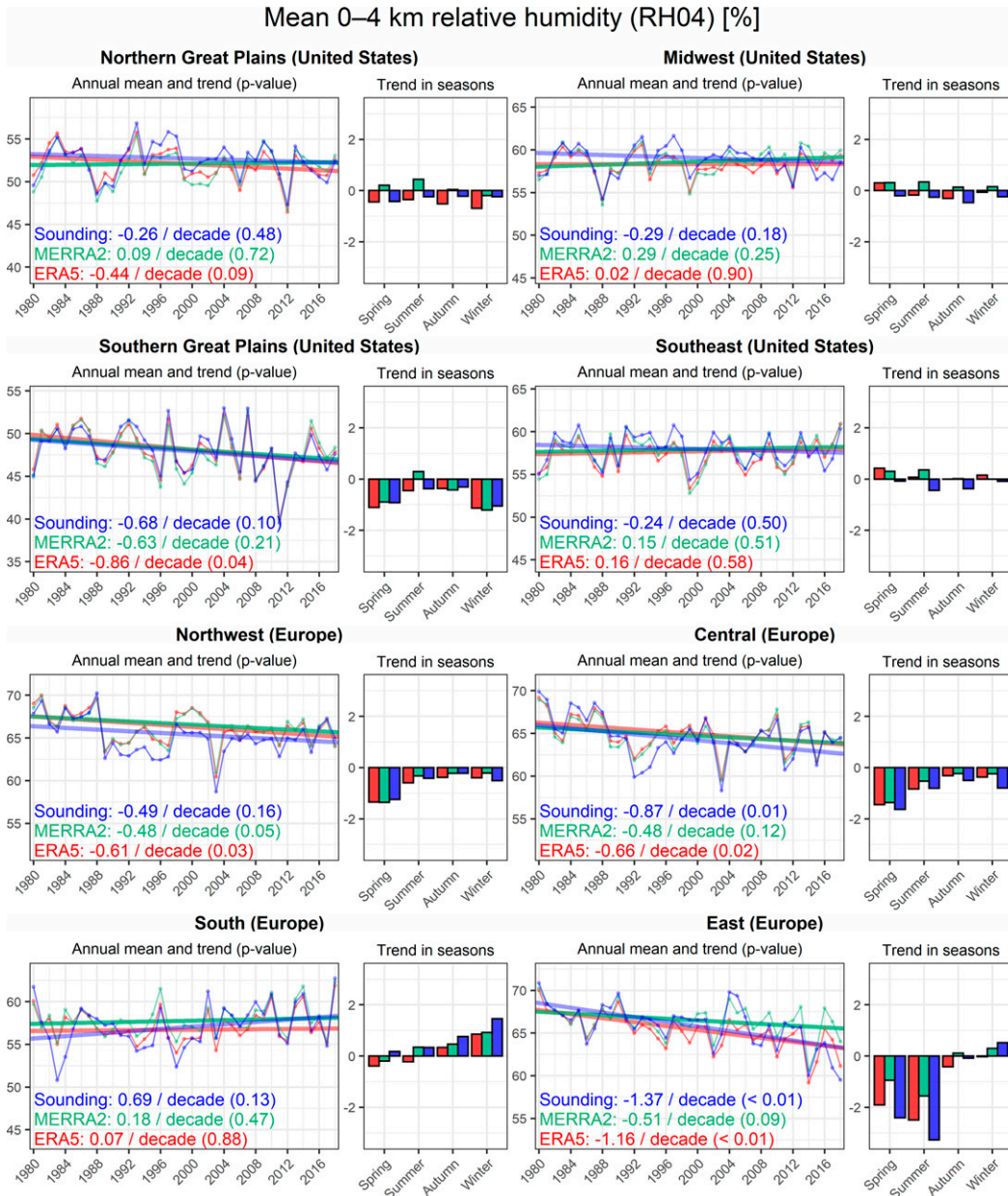


FIG. 5. As in Fig. 3, but for mean 0–4-km relative humidity.

indicates strong decreases in contrast to ERA5 and soundings. Over both domains ERA5 provides overall similarity to soundings for LR03 as compared with MERRA-2, which is mostly underestimated. Although the biggest differences among datasets are observed over southern Europe, the slope of the trend is very similar.

Consistent decreases in the mean 0–4-km AGL relative humidity (RH04) are observed for both continents and each dataset (Fig. 2c). This result is in line with prior studies suggesting that pronounced decreases in the land surface relative humidity are an expected outcome of a warming climate as temperature rises outpace available moisture (Frick et al.

2014; Byrne and O’Gorman 2016, 2018; Vicente-Serrano et al. 2018; Chen et al. 2020; Taszarek et al. 2021a). Across the southern Great Plains all datasets suggest reductions in RH04 of around -1% per decade during spring and winter, while over other regions in the United States only modest and insignificant signals are observed (Fig. 5).

In Europe, trends in RH04 are more mixed depending on the region and season evaluated. Significant decreases in all seasons are found across the datasets for central, eastern, and northwestern Europe. Annual rates of change exceed -0.5% per decade, and the strongest decreases above -2% per decade are in spring and summer (Fig. 5). The most significant

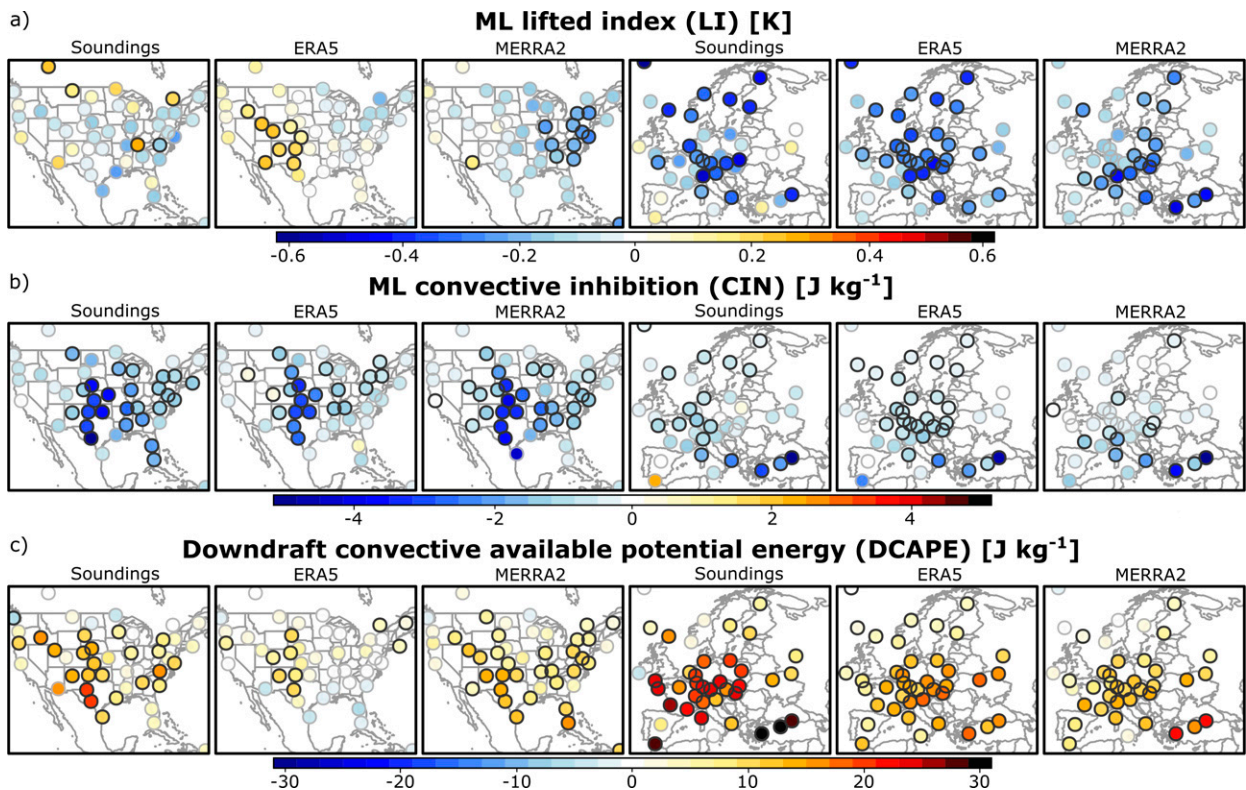


FIG. 6. As in Fig. 2, but for (a) ML lifted index, (b) ML convective inhibition, and (c) downdraft convective available potential energy.

changes can be observed especially in eastern Europe, where all datasets are in agreement with downward trends. In contrast, changes over southern Europe indicate increases, mainly during autumn and winter, but these signals are mostly insignificant.

b. Buoyancy parameters

Spatial patterns in trends of LI are similar to MIXR with all datasets having a consistent signal across Europe, and different signals in the United States. While changes to instability based on sounding data seems to be mostly insignificant, ERA5 indicates significant decreases in buoyancy (increases in LI) over the western mountainous part of the United States (Fig. 6a). MERRA-2 has a differing pattern with robust increases to buoyancy (decreases in LI) observed over the eastern portion of the United States. Seasonally, trends among the datasets and seasons are mixed with the most consistent changes over the Midwest where increases in buoyancy are observed in summer and autumn (Fig. 7). In comparison with these results, DeRubertis (2006) using rawinsonde observations over the period 1973–97 found an increase in instability during summer, particularly over the southern states.

In Europe, the atmosphere has become significantly more unstable across all datasets, with the most notable decreases in LI over parts of central and southern Europe, especially in the Alpine region where the rate of change exceeds -0.5 K per decade (Fig. 6a). Seasonal changes in Europe are also consistent between datasets and indicate consistent increases

in instability in every season and region (except spring and summer in eastern Europe; Fig. 7). Another important aspect is that over the entire evaluated 39-yr period mean errors between reanalyses and soundings are small, despite inconsistency in dewpoints caused by changes in the instrumentation around the year 1990 (Mohr and Kunz 2013). These cross-dataset findings for LI increases our confidence in the result of consistently increasing atmospheric instability across Europe, mainly driven by rising near-surface temperature and moisture (Kunz et al. 2009; Riemann-Campe et al. 2009; Púčik et al. 2017; Rädler et al. 2019; Taszarek et al. 2021a). However, as noted in prior research, increases to moisture provide more near-surface moist static energy and thus deliver a greater contribution to rising instability (Agard and Emanuel 2017; Li and Chavas 2021).

Despite differences among moisture and instability parameters between reanalyses and observations over the United States, there is robust agreement for changes in CIN. CIN is a very important variable that, when large in magnitude, is indicative of resistance of the atmosphere to storm initiation, despite the availability of ample instability (Wilson and Roberts 2006; Bunkers et al. 2010; Gensini and Ashley 2011; Hoogewind et al. 2017; Westermayer et al. 2017; Taszarek et al. 2020b). Over both domains each of the datasets shows robust decreases in CIN (increasing inhibition) (Fig. 6b). Across the United States, the highest decreases in CIN occur over the Great Plains (around -3.5 J kg⁻¹ per decade) where climatologically CIN reaches the highest values (Gensini and

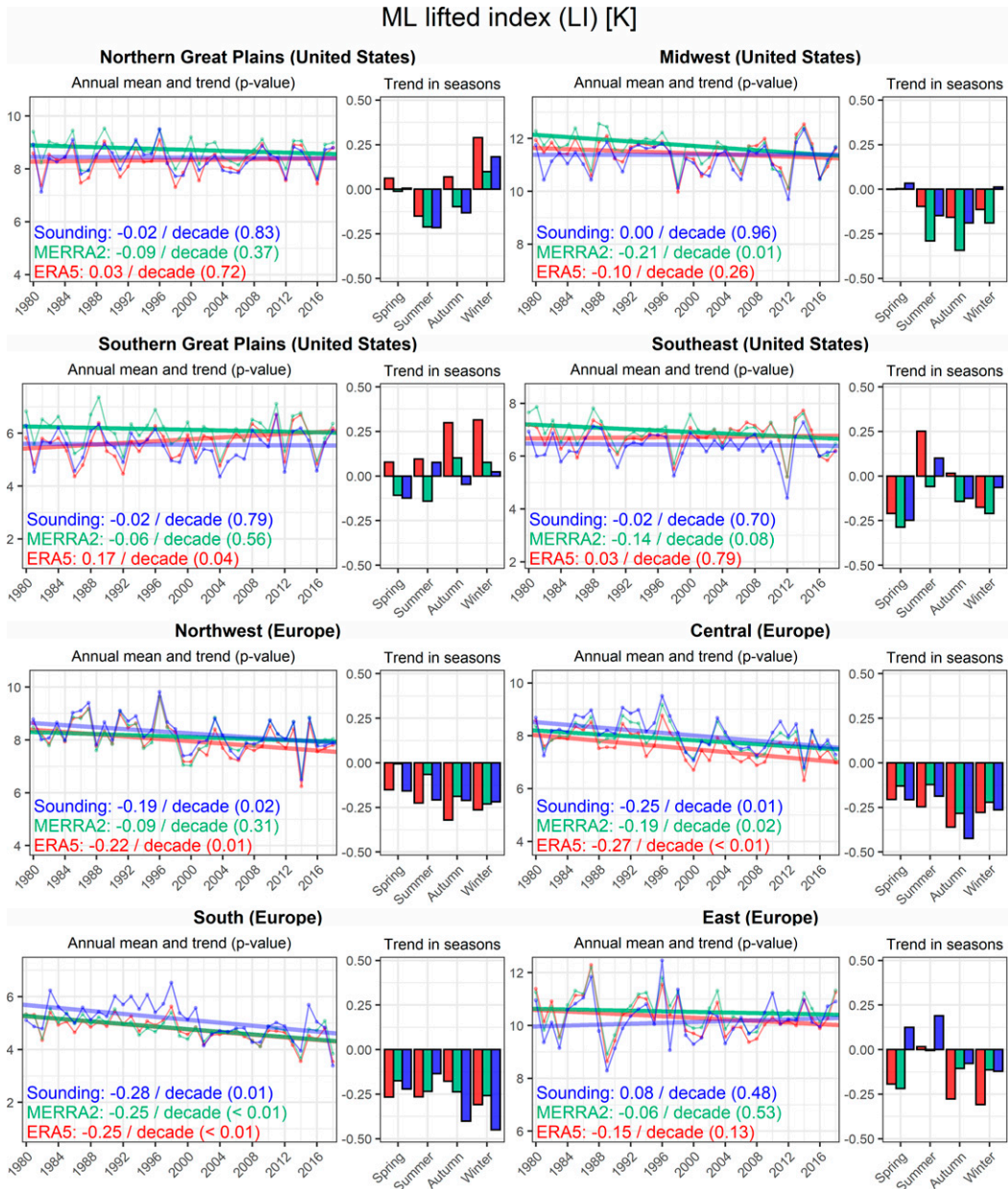


FIG. 7. As in Fig. 3, but for ML lifted index.

Ashley 2011; Taszarek et al. 2020b). However, significant decreases in CIN are found at almost every station east of the Rocky Mountains, suggesting increasing resistance to convection and greater stability (Figs. 6b and 8). Decreases in CIN are found for all seasons, but the strongest rate of change of around -5 J kg^{-1} per decade is during spring and summer across the Great Plains. Although the slope of the trend is generally in good agreement with observations, reanalyses still underestimate the absolute value of CIN (Fig. 8). Results also indicate that consistent increases in convective inhibition seem to be advancing faster than changes to instability, which may lead to less effective convective initiation in the future—a

result that is broadly consistent with prior studies (Hoogewind et al. 2017; Chen et al. 2020; Rasmussen et al. 2020; Taszarek et al. 2021a).

In Europe, changes to CIN are less pronounced, partly as a result of overall smaller climatological CIN (Siedlecki 2009), but the rate and sign of change remains consistent between reanalyses and soundings (Fig. 6b). Trends for Europe generally do not fall below -1 J kg^{-1} per decade, although the majority of these signals are still significant. Seasonally, the largest decreases in CIN (increasing inhibition) occur during both spring and summer over southern Europe, while changes elsewhere during the remainder of the year are very small and

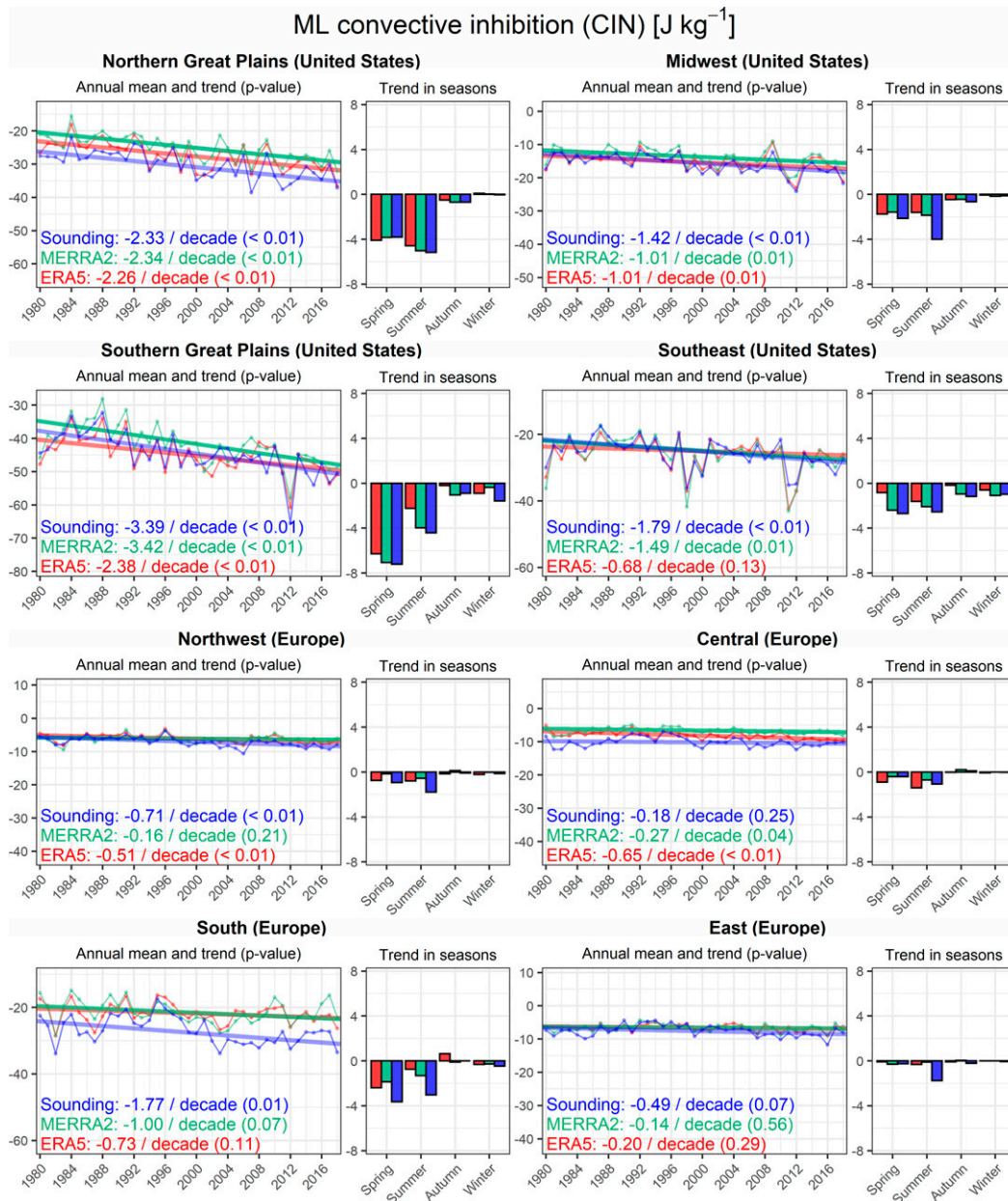


FIG. 8. As in Fig. 3, but for ML convective inhibition.

not significant (Fig. 8). Similar to the United States, both ERA5 and MERRA-2 demonstrate a consistent underestimation of CIN through time for Europe. However, in contrast to LI, reanalyses successfully reconstruct the rate of the change and sign over both domains; regardless of the analyzed region, the largest changes are typically during spring and summer (Fig. 8).

Another parameter of interest is DCAPE—a proxy of atmospheric potential for producing strong convective winds originating from evaporative cooling of downdrafts (Gilmore and Wicker 1998). Values of DCAPE are generally large when the midtroposphere is dry and low-level

lapse rates are steep. Thus, previously discussed decreases in RH04 (Fig. 6c) and increases in LR03 (Fig. 6b) should lead to higher DCAPE over time. Although large instability environments are typically accompanied also by high DCAPE, as evidenced in our study, trends in these parameters are not consistent. Despite mixed trends in LI across the United States (Fig. 6a), reanalyses and soundings are in better agreement in terms of significant increases to DCAPE over the United States (Fig. 6c). Positive trends are also found for every season and region with the most significant changes during spring and summer across the Great Plains of the United States (Fig. 9).

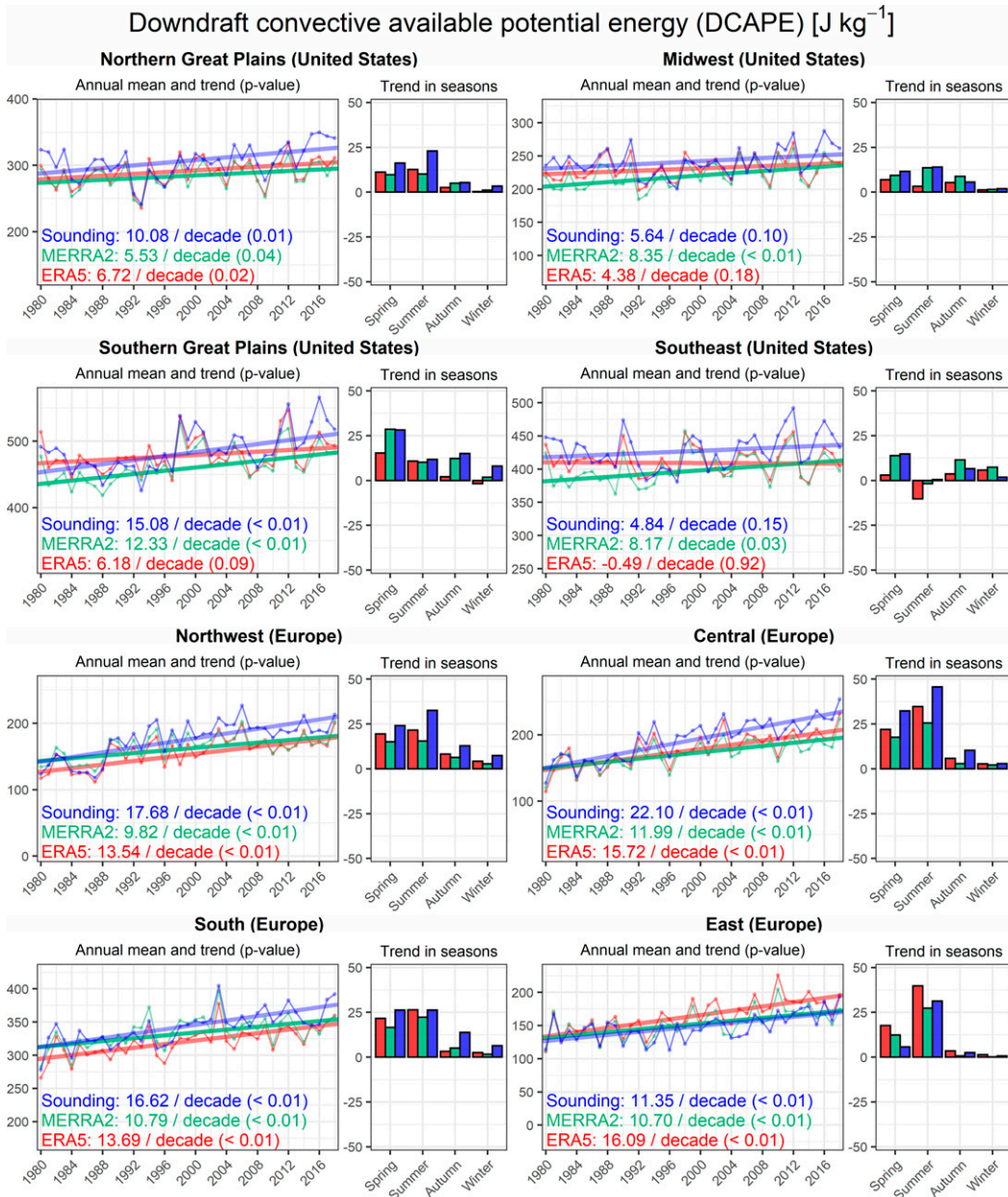


FIG. 9. As in Fig. 3, but for downdraft convective available potential energy.

In Europe, robust increases in DCAPE can be found across the entire continent, each dataset, and every season (Figs. 6c and 9). The highest rate of change in the mean annual DCAPE is observed over southern Europe with some of the sounding stations indicating increases as large as $+30 \text{ J kg}^{-1}$ per decade. Changes in central and western Europe are also pronounced with many stations exceeding $+25 \text{ J kg}^{-1}$ per decade. The highest contribution to these increases is mainly during summer in line with the annual cycle of convective activity, but also in spring (Fig. 9). These results indicate that the potential for severe convective winds resulting from evaporative cooling of the downdrafts is increasing across Europe.

Whether this has manifested in observed downburst events is difficult to assess as there remain strong temporal and spatial limitations for wind reports in the European Severe Weather Database (Pacey et al. 2021). It is also important to highlight that over both domains, reanalyses mostly underestimate absolute values of DCAPE when compared with soundings (Fig. 9).

c. Wind parameters

Changes in the vertical profile of wind are an important aspect of convective environments, as availability of strong

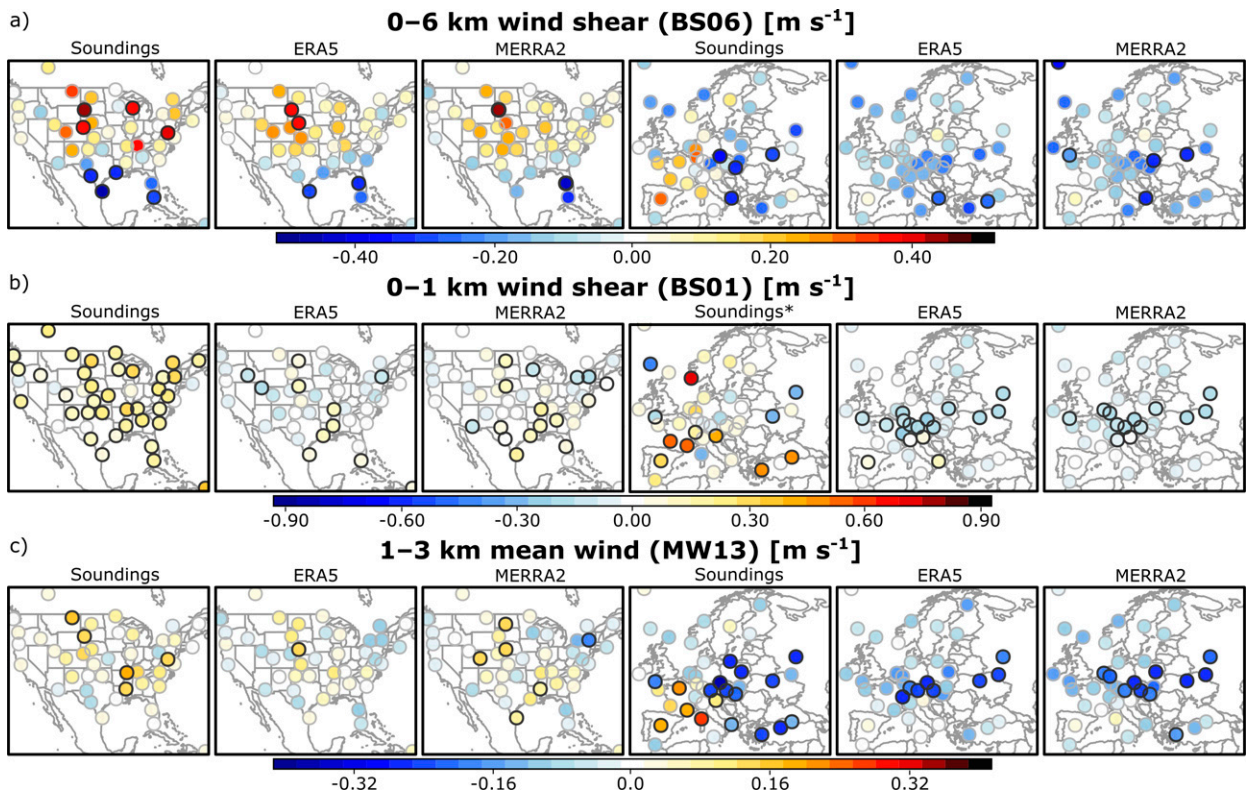


FIG. 10. As in Fig. 2, but for (a) 0–6-km wind shear, (b) 0–1-km wind shear, and (c) 1–3-km mean wind. Sounding trends for regions marked with an asterisk cover the period of 1992–2018 (see section 3c for further details).

vertical wind shear and/or the presence of a low-level jet promotes better organized convective modes such as squall lines or supercells that are more capable of producing severe weather (Smith et al. 2012; Thompson et al. 2012; Guastini and Bosart 2016; Bagagnini et al. 2021; Pacey et al. 2021). Changes to BS06 over both domains are generally modest with most trends being insignificant (Fig. 10a). However, despite the low mean errors for wind parameters, the slope of the trend and sign is diversified among seasons and regions (Fig. 11). The most consistent signal among all datasets is observed over the northern Great Plains and the Midwest where a mean annual BS06 has been increasing with a rate of around $+0.2 \text{ m s}^{-1}$ per decade, mostly during spring and winter (Fig. 11). In Europe, a long-term decrease occurs in almost every season and in each dataset except northwest where increases in the sounding database (mostly during winter) are in contrast to modest decreases in ERA5 and MERRA-2 (Fig. 10). Better overlap between absolute values of BS06 in soundings and reanalysis is observed in the United States as compared with Europe, although both reanalyses typically underestimate BS06.

Considerable differences between observations and reanalyses are found for BS01, an important parameter in tornado prediction (Thompson et al. 2003; Grams et al. 2012; Gensini and Bravo de Guenni 2019; Ingrassio et al. 2020; Rodríguez and Bech 2020; Tochimoto et al. 2021). This is somewhat unsurprising given a known tendency for this parameter to be

underestimated in numerical weather prediction datasets (Allen and Karoly 2014; Gensini et al. 2014; Taszarek et al. 2018; King and Kennedy 2019; Taszarek et al. 2021b). Our results indicate not only large differences in the absolute values of BS01 between the datasets, but also differing signs of the trend for soundings (Figs. 10b and 12). The two reanalyses provide generally very similar signals, with local modest significant increases across the United States and decreases in Europe, while soundings over both continents feature increases, which are the largest over southwestern Europe (Figs. 10b and 12). For Europe, the mean error in BS01 between reanalyses and soundings has changed over time from overestimation in the 1980s to underestimation in recent years with respect to ERA5. This tendency may be connected with a changing quality of rawinsonde wind measurements over time, and an increasing number of available low-tropospheric levels in the 1990s for the area of Europe (Taszarek et al. 2021b). Using the “Standard Normal Homogeneity Test” (the *R trend* package), we found a changepoint in BS01 data in 1992 for all analyzed European regions. Because of that clear discontinuity, we present trends for soundings in Europe for the period of 1992–2018 (Figs. 10 and 12). For these years both reanalyses have similar trend slopes as sounding data across southern and eastern Europe but feature higher underestimation of BS01 absolute values when compared with the United States.

Considering a mean wind in the 1–3-km AGL layer (MW13) as proxy for the low-level jet (Rife et al. 2010;

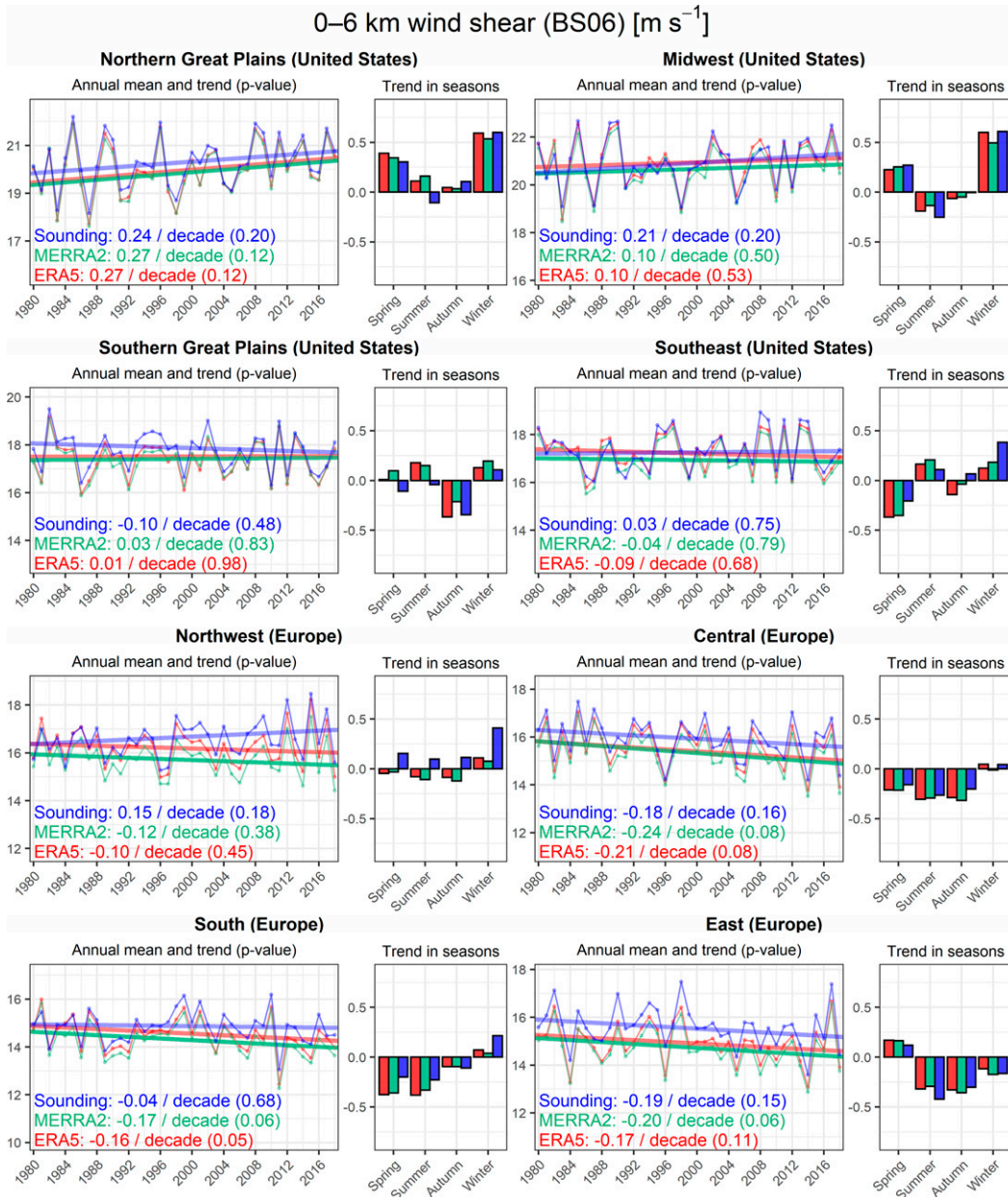


FIG. 11. As in Fig. 3, but for 0–6-km wind shear.

Shapiro et al. 2016), we find more consistent results between datasets as compared with BS01 (Fig. 10). Trends in MW13 across the United States are mixed seasonally, but those stations that exhibit significant changes indicate small increases over the Southeast (mainly during summer and winter; Fig. 13). Changes to MW13 across Europe are spatially very similar to those of BS06, with more widespread significant trends (Fig. 10c). Sounding trends are mixed, while reanalyses seem to only capture negative trends with the biggest differences relative to observations over southwestern Europe. Consistent significant decreases in MW13 are found for all datasets over central and eastern Europe in every season (Fig. 13). In

contrast to BS01, MW13 features fairly small mean errors in magnitude between soundings and reanalyses, although errors are similarly larger over Europe (Fig. 13).

d. Vertical profiles

To better understand which processes are leading to specific changes in convective parameters, we evaluate trends in vertical profiles of temperature in all three datasets. In the United States (Fig. 14), positive trends in air temperature across the vertical profile can be observed during all seasons except winter. Temperature increases generally by around 0.2°C per decade, but this rate differs among regions and by

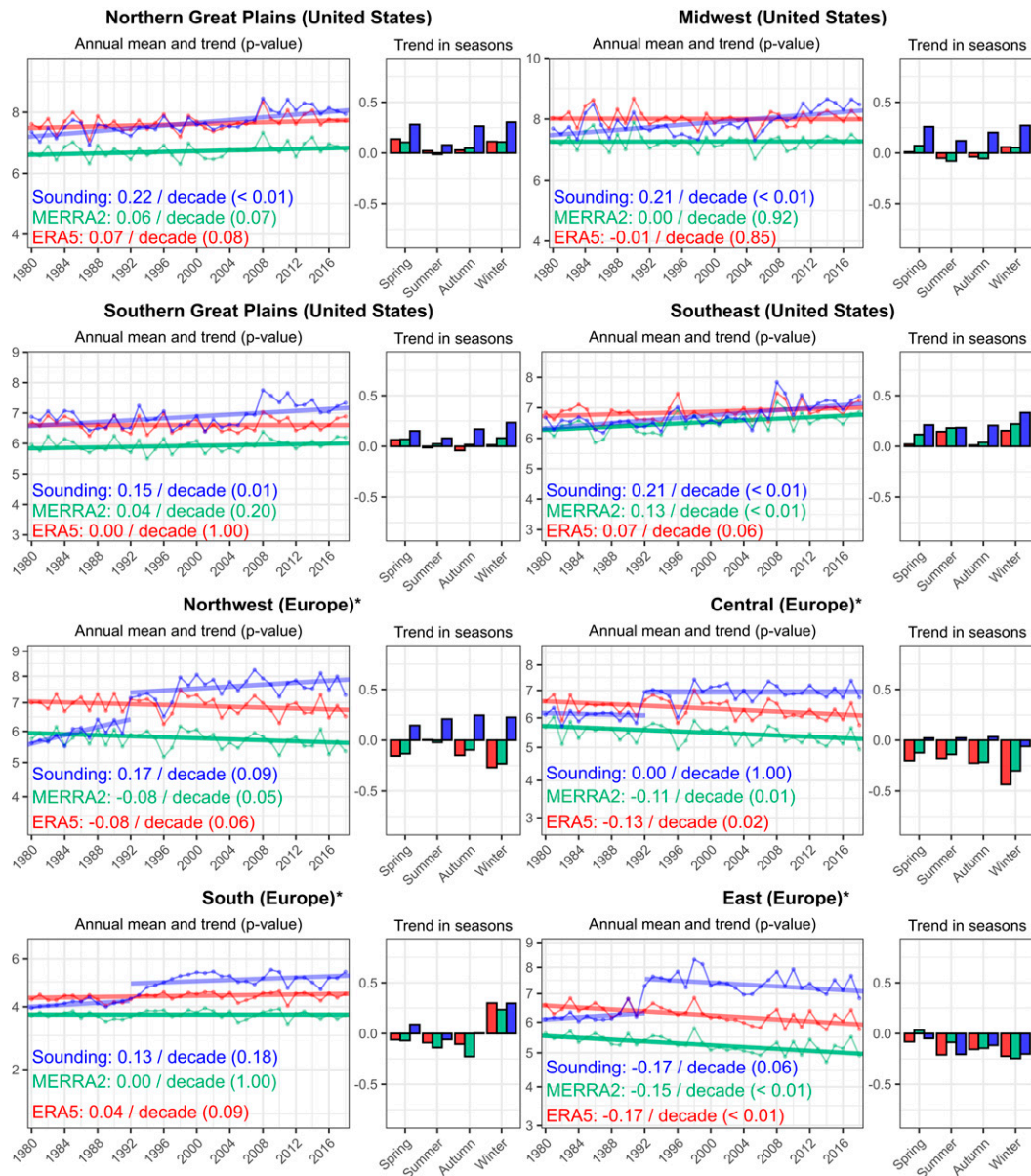
0–1 km wind shear (BS01) [m s^{-1}]

FIG. 12. As in Fig. 3, but for 0–1-km wind shear. Sounding trends for regions marked with an asterisk cover the period of 1992–2018 (see section 3c for further details).

AGL height (Fig. 14). The best agreement among datasets in terms of significance of the trend is observed across the southern Great Plains in spring, summer, and autumn, when warming of the near surface is lower relative to aloft. This pattern may be related to more intense drying and warming over the western United States, which through the advection of elevated mixed layers, is displaced eastward (Carlson and Ludlam 1968). As evidenced in the results of our study, this mechanism leads to increases in CIN, and in some situations may even cause stabilization and decreases in instability (Taszarek et al. 2021a). The biggest differences among the datasets are during

winter, especially over the northern Great Plains and the Midwest where sounding measurements indicate negative trends in low and middle troposphere as opposed to modest changes in ERA5 and MERRA-2 (Fig. 14).

In Europe, we find a good agreement between datasets among all regions and seasons, except spring and summer over eastern Europe where sounding data indicate faster warming as compared with ERA5 and MERRA-2 (Fig. 15). Increases in temperature of around $+0.5^{\circ}\text{C}$ per decade in almost the entire tropospheric profile are significant among datasets during spring and summer across northwestern,

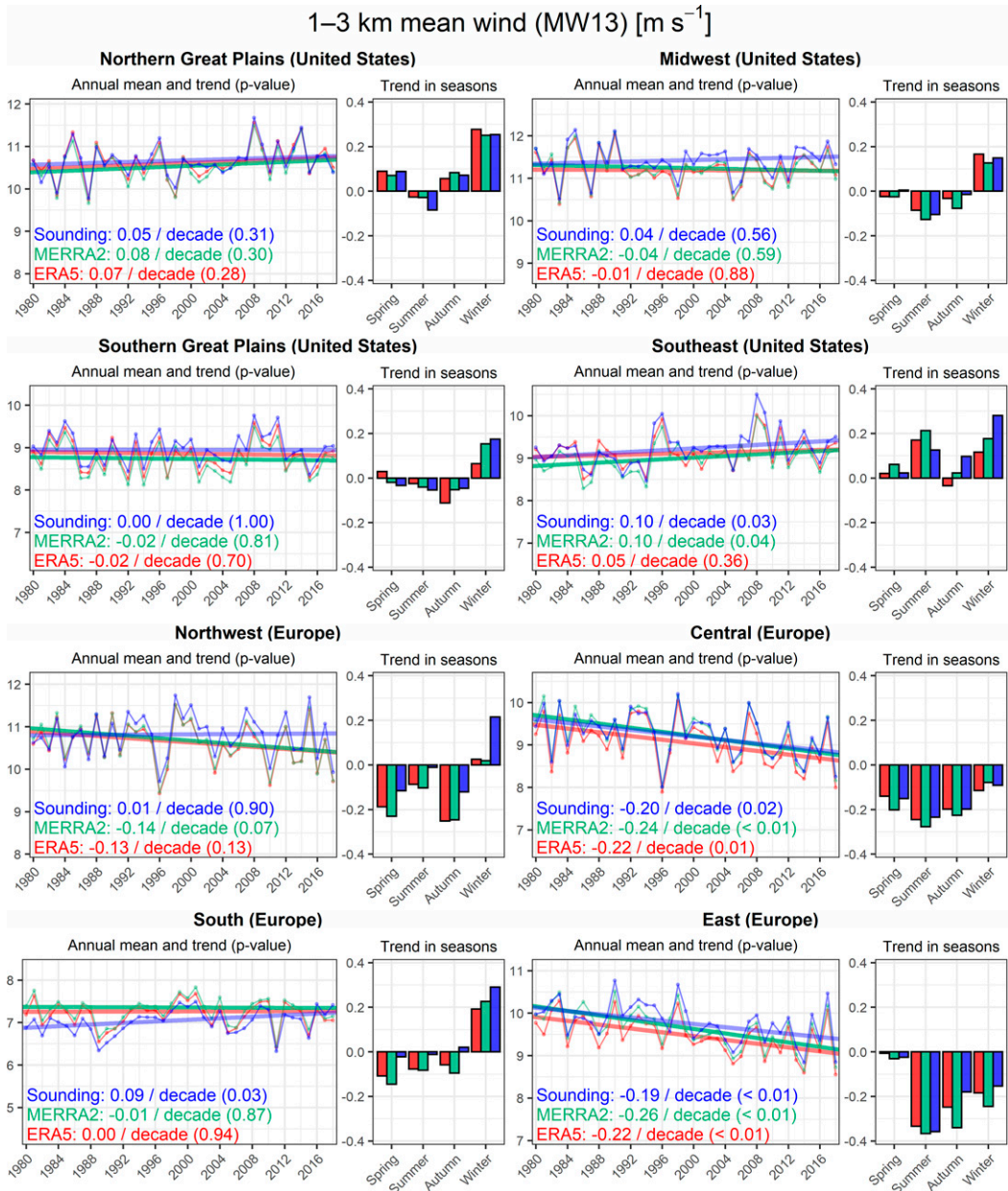


FIG. 13. As in Fig. 3, but for 1–3-km mean wind.

central, and southern Europe, and summer and autumn in eastern Europe. In autumn and winter, trends across northwestern, central, and southern Europe have typically smaller and insignificant rates with the highest values near surface (Fig. 15). It can be also observed that for both Europe and the United States the rate of warming in the upper troposphere decreases with height and in some regions negative trend values occur, especially for the sounding data. This finding is in agreement with IPCC reports, where cooling of the upper troposphere and stratosphere over the last decades has also been indicated (IPCC 2014).

4. Concluding remarks and discussion

In this study trends in convective parameters derived from ERA5 and MERRA-2 reanalyses were compared with ~ 2.07 million proximal atmospheric soundings over the period of 39 years (1980–2018) across Europe and the United States. We examined which parameters commonly used in the operational prediction of severe thunderstorms and climatological evaluations feature consistent trends among datasets and which have differing signals. Results consistent among soundings, ERA5 and MERRA-2 increase our confidence while

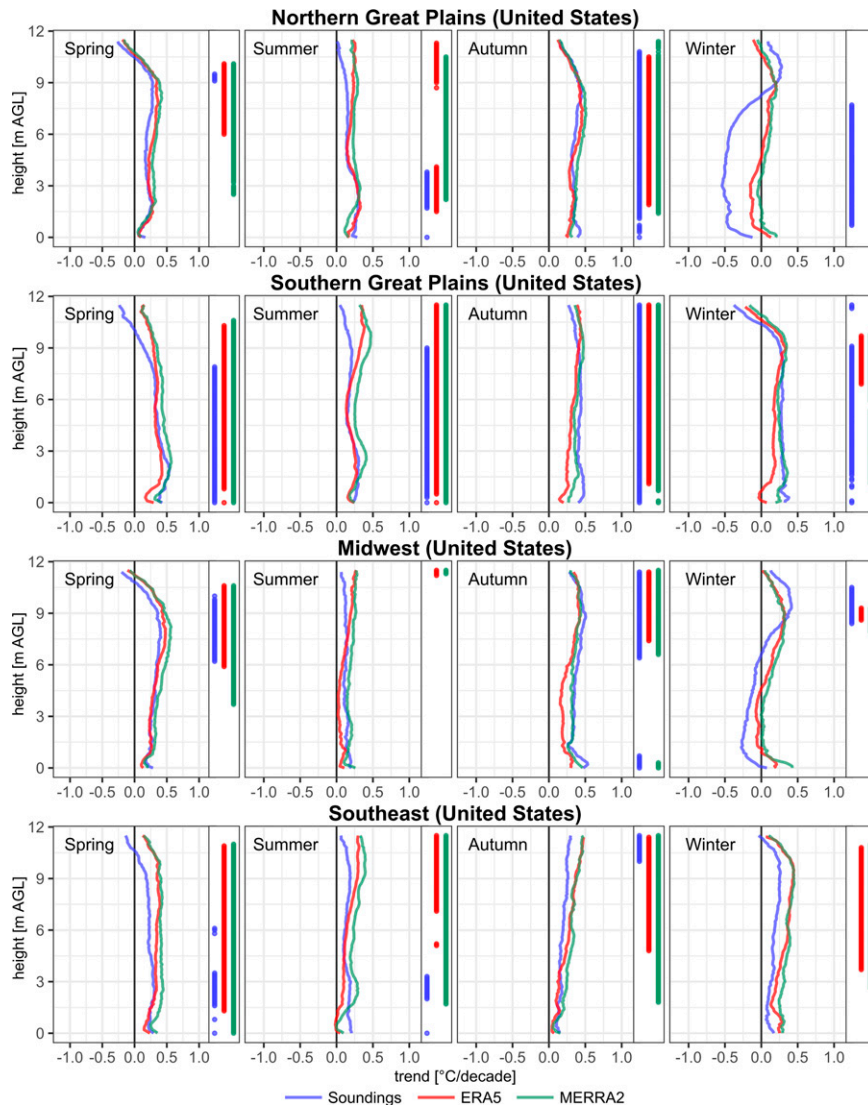


FIG. 14. Long-term trends of air temperature at specific heights AGL based on the period 1980–2018 and across the United States. Trend is derived from Sen's slope. Points on the right side of each plot denote layers with trends that have two-tailed p values below 0.05.

differences raise uncertainties. Below, we highlight the most important findings:

- Differences in trends exist between Europe and the United States for common metrics including low-level moisture, lapse rates, instability, vertical wind shear, and mean wind. These differences are robust whether using observations or reanalysis data.
- Trends seem to be more consistent among reanalyses and sounding datasets over Europe as compared with the United States where bigger differences are observed for MERRA-2 in low-level moisture and instability.
- All datasets are in a remarkable agreement for trends in CIN. This highlights robust strengthening of inhibition through differential midtropospheric warming, especially across the Great Plains during spring and summer despite only modest changes to instability.
- Robust increases in DCAPE are consistent among datasets and domains. These changes indicate that the potential for severe winds resulting from evaporative cooling is likely increasing in a warming climate as low-level lapse rates are becoming steeper and relative humidity decreases, thus contributing to higher DCAPE.
- Low-level wind shear features clear data inhomogeneities over time for sounding measurements. Reanalyses indicate modest increases over the United States and decreases in Europe, while soundings indicate increases over both domains. This disagreement indicates large uncertainties related to trends in BS01. Low correlations and enhanced mean errors for this parameter were also found in prior

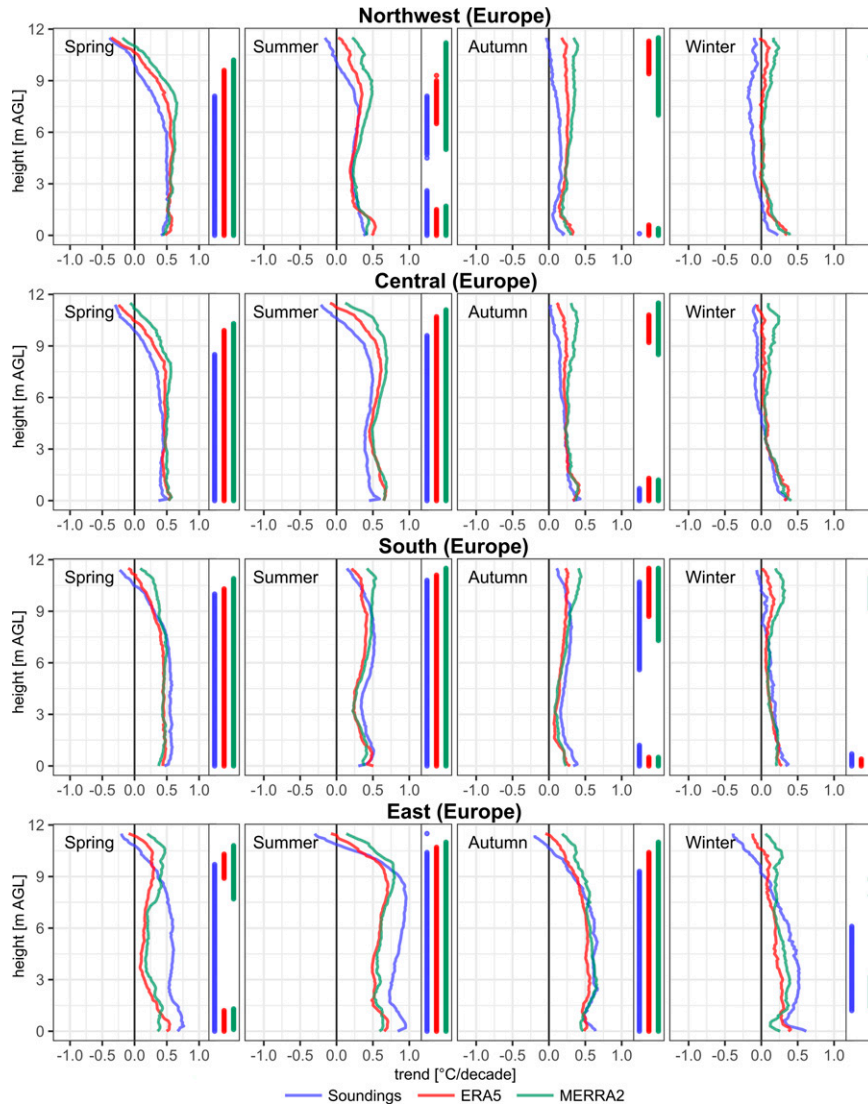


FIG. 15. As in Fig. 14, but for Europe.

studies comparing reanalyses with observations (Allen and Karoly 2014; Gensini et al. 2014; Tazarek et al. 2018; King and Kennedy 2019; Tazarek et al. 2021b).

- Reanalyses are in a good agreement with observations for trends in deep-layer wind shear and low-level jet, although these trends are generally insignificant. Modest increases are observed across the United States while reductions occur in Europe. This result remains in contrast to future projections evaluated in Hoogewind et al. (2017) and Rädler et al. (2018) where opposite signals for the vertical wind shear were found. However, it is possible that projected trends may not have emerged from relatively larger interannual variability.
- Trends in vertical profiles of air temperature represented by soundings, ERA5, and MERRA-2 show warming of the low and middle troposphere for almost all seasons and regions. Significant changes were found for all seasons in

the southern Great Plains, as also for spring and summer in all European regions. In Europe warming is the strongest typically near surface while in the United States around 2–3 km AGL, which contributes to increases in CIN.

Results presented in this study suggest that while trends may vary depending on evaluated variable and region, reanalyses are generally capable of providing reasonable results for convective parameters when used with caution. While this differs from the overall aim of reanalysis products (Thorne and Vose 2010), these offer much better temporal and spatial record than observations for this application and thus can be used in more complex analyses. As recent reanalyses have become increasingly popular in studying convective environments (e.g., Gensini and Brooks 2018; Rädler et al. 2018; Mohr et al. 2019; Tang et al. 2019; Tippet et al. 2019; Li et al. 2020; Bagaglini et al. 2021; Sulik 2021), it is of great importance to test their

performance and be aware of their limitations. However, given the limitations of observational data, soundings should be also used with caution as a reference dataset. While ERA5 and MERRA-2 differ in terms of spatial resolution or assimilation methods used in their production, trends evaluated in this study are similar for many variables and indicate a similar sign of change when compared with observations. This similarity is most prevalent for CIN, DCAPE, BS06, and MW13, where spatial variability, statistical significance, and the magnitude of trends is consistent between the datasets.

Near-ground wind and moisture parameters continue to present issues for credible trend evaluation, with notable discrepancies among datasets for parameters like MIXR over the United States and BS01 in Europe. This trend inconsistency is despite high correlations exceeding 0.97 for MIXR when ERA5 and MERRA-2 are compared with soundings (Taszarek et al. 2021b). This highlights that statistically significant correlations may not necessarily mean that a reanalysis has a credible representation of a long-term trend as the skill of reanalyses and reliability of rawinsonde measurements also changes over time. Not every dataset may be suitable for reliable sampling of trends in selected variables or geographical regions and thus any results considering temporal changes should be always interpreted with caution and compared with available datasets. As shown in our study, a good agreement among datasets for CIN and DCAPE increased our confidence for trends in these parameters, while differences for MIXR or BS01 raised uncertainties.

Acknowledgments. This research was supported by grants from the Polish National Science Centre (2017/27/B/ST10/00297 and 2019/33/N/ST10/00403). Author J. T. Allen acknowledges support from the National Science Foundation under Grant AGS-1945286. Additional funding was provided by the NOAA/Office of Oceanic and Atmospheric Research under NOAA–University of Oklahoma Cooperative Agreement NA16OAR4320115 and NOAA–University of Oklahoma Cooperative Agreement NA21OAR4320204, U.S. Department of Commerce. The reanalysis computations were performed in the Poznań Supercomputing and Networking Center (project 448).

Data availability statement. All datasets used in this study are openly available. ERA5 data were downloaded from the European Centre for Medium-Range Weather Forecasts (ECMWF) via Copernicus Climate Change Service (C3S; <https://cds.climate.copernicus.eu/>). MERRA-2 data were downloaded from the National Aeronautics and Space Administration (NASA) Goddard Earth Sciences Data and Information Services Center (GES DISC; <https://disc.gsfc.nasa.gov/>). Radiosonde data were downloaded from the University of Wyoming upper-air database (<http://weather.uwyo.edu/upperair/>).

REFERENCES

- Agard, V., and K. Emanuel, 2017: Clausius–Clapeyron scaling of peak CAPE in continental convective storm environments. *J. Atmos. Sci.*, **74**, 3043–3054, <https://doi.org/10.1175/JAS-D-16-0352.1>.
- Alghamdi, A. S., 2020: Evaluation of four reanalysis datasets against radiosonde over southwest Asia. *Atmosphere*, **11**, 402, <https://doi.org/10.3390/atmos11040402>.
- Allen, J. T., 2018: Climate change and severe thunderstorms. *Oxford Research Encyclopedia of Climate Science*, Oxford University Press, 516 pp., <https://doi.org/10.1093/acrefore/9780190228620.013.62>.
- , and D. J. Karoly, 2014: A climatology of Australian severe thunderstorm environments 1979–2011: Inter-annual variability and ENSO influence. *Int. J. Climatol.*, **34**, 81–97, <https://doi.org/10.1002/joc.3667>.
- , and M. K. Tippett, 2015: The characteristics of United States hail reports: 1955–2014. *Electron. J. Severe Storms Meteor.*, **10** (3), <https://ejssm.com/ojs/index.php/site/article/view/60/59>.
- , D. J. Karoly, and K. J. Walsh, 2014: Future Australian severe thunderstorm environments. Part I: A novel evaluation and climatology of convective parameters from two climate models for the late twentieth century. *J. Climate*, **27**, 3827–3847, <https://doi.org/10.1175/JCLI-D-13-00425.1>.
- Bagalini, L., R. Inghrosso, and M. M. Miglietta, 2021: Synoptic patterns and mesoscale precursors of Italian tornadoes. *Atmos. Res.*, **253**, 105503, <https://doi.org/10.1016/j.atmosres.2021.105503>.
- Bao, X., and F. Zhang, 2019: How accurate are modern atmospheric reanalyses for the data-sparse Tibetan Plateau region? *J. Climate*, **32**, 7153–7172, <https://doi.org/10.1175/JCLI-D-18-0705.1>.
- Barandiaran, D., S.-Y. Wang, and K. Hilburn, 2013: Observed trends in the Great Plains low-level jet and associated precipitation changes in relation to recent droughts. *Geophys. Res. Lett.*, **40**, 6247–6251, <https://doi.org/10.1002/2013GL058296>.
- Brown, T. M., W. H. Pogorzelski, and I. M. Giammanco, 2015: Evaluating hail damage using property insurance claims data. *Wea. Climate Soc.*, **7**, 197–210, <https://doi.org/10.1175/WCAS-D-15-0011.1>.
- Bunkers, M. J., J. R. Wetenkamp, J. J. Schild, and A. Fischer, 2010: Observations of the relationship between 700-mb temperatures and severe weather reports across the contiguous United States. *Wea. Forecasting*, **25**, 799–814, <https://doi.org/10.1175/2009WAF2222333.1>.
- Byrne, M. P., and P. A. O’Gorman, 2016: Understanding decreases in land relative humidity with global warming: Conceptual model and GCM simulations. *J. Climate*, **29**, 9045–9061, <https://doi.org/10.1175/JCLI-D-16-0351.1>.
- , and —, 2018: Trends in continental temperature and humidity directly linked to ocean warming. *Proc. Natl. Acad. Sci. USA*, **115**, 4863–4868, <https://doi.org/10.1073/pnas.1722312115>.
- Carlson, T. N., and F. H. Ludlam, 1968: Conditions for the occurrence of severe local storms. *Tellus*, **20**, 203–226, <https://doi.org/10.3402/tellusa.v20i2.10002>.
- Chen, J., A. Dai, Y. Zhang, and K. L. Rasmussen, 2020: Changes in convective available potential energy and convective inhibition under global warming. *J. Climate*, **33**, 2025–2050, <https://doi.org/10.1175/JCLI-D-19-0461.1>.
- Coniglio, M. C., and M. D. Parker, 2020: Insights into supercells and their environments from three decades of targeted radiosonde observations. *Mon. Wea. Rev.*, **148**, 4893–4915, <https://doi.org/10.1175/MWR-D-20-0105.1>.
- Copernicus Climate Change Service, 2017: ERA5: Fifth generation of ECMWF atmospheric reanalyses of the global climate. Copernicus Climate Change Service Climate Data

- Store (CDS), accessed 2 December 2020, <https://cds.climate.copernicus.eu/cdsapp#!/home>.
- Craven, J. P., and H. E. Brooks, 2004: Baseline climatology of sounding derived parameters associated with deep moist convection. *Natl. Wea. Dig.*, **28**, 13–24, <http://nwafiles.nwas.org/digest/papers/2004/Vol28/Pg13-Craven.pdf>.
- DeRubertis, D., 2006: Recent trends in four common stability indices derived from U.S. radiosonde observations. *J. Climate*, **19**, 309–323, <https://doi.org/10.1175/JCLI3626.1>.
- Diffenbaugh, N. S., F. Giorgi, L. Raymond, and X. Bi, 2007: Indicators of 21st century socioclimatic exposure. *Proc. Natl. Acad. Sci. USA*, **104**, 20195–20198, <https://doi.org/10.1073/pnas.0706680105>.
- , M. Scherer, and R. J. Trapp, 2013: Robust increases in severe thunderstorm environments in response to greenhouse forcing. *Proc. Natl. Acad. Sci. USA*, **110**, 16361–16366, <https://doi.org/10.1073/pnas.1307758110>.
- Doswell, C. A., H. E. Brooks, and M. P. Kay, 2005: Climatological estimates of daily local nontornadic severe thunderstorm probability for the United States. *Wea. Forecasting*, **20**, 577–595, <https://doi.org/10.1175/WAF866.1>.
- Edwards, R., J. T. Allen, and G. W. Carbin, 2018: Reliability and climatological impacts of convective wind estimations. *J. Appl. Meteor. Climatol.*, **57**, 1825–1845, <https://doi.org/10.1175/JAMC-D-17-0306.1>.
- Frick, C., H. Steiner, A. Mazurkiewicz, U. Riediger, M. Rauthe, T. Reich, and A. Gratzki, 2014: Central European high-resolution gridded daily data sets (HYRAS): Mean temperature and relative humidity. *Meteor. Z.*, **23**, 15–32, <https://doi.org/10.1127/0941-2948/2014/0560>.
- Gelaro, R., and Coauthors, 2017: The Modern-Era Retrospective Analysis for Research and Applications, version 2 (MERRA-2). *J. Climate*, **30**, 5419–5454, <https://doi.org/10.1175/JCLI-D-16-0758.1>.
- Gensini, V. A., and W. S. Ashley, 2011: Climatology of potentially severe convective environments from the North American Regional Reanalysis. *Electron. J. Severe Storms Meteor.*, **6** (8), <https://ejssm.com/ojs/index.php/site/article/view/35/35>.
- , and T. L. Mote, 2015: Downscaled estimates of late 21st century severe weather from CCSM3. *Climatic Change*, **129**, 307–321, <https://doi.org/10.1007/s10584-014-1320-z>.
- , and H. E. Brooks, 2018: Spatial trends in United States tornado frequency. *npj Climate Atmos. Sci.*, **1**, 38, <https://doi.org/10.1038/s41612-018-0048-2>.
- , and L. Bravo de Guenni, 2019: Environmental covariate representation of seasonal U.S. tornado frequency. *J. Appl. Meteor. Climatol.*, **58**, 1353–1367, <https://doi.org/10.1175/JAMC-D-18-0305.1>.
- , T. L. Mote, and H. E. Brooks, 2014: Severe-thunderstorm reanalysis environments and collocated radiosonde observations. *J. Appl. Meteor. Climatol.*, **53**, 742–751, <https://doi.org/10.1175/JAMC-D-13-0263.1>.
- Gilmore, M. S., and L. J. Wicker, 1998: The influence of midtropospheric dryness on supercell morphology and evolution. *Mon. Wea. Rev.*, **126**, 943–958, [https://doi.org/10.1175/1520-0493\(1998\)126<0943:TIOMDO>2.0.CO;2](https://doi.org/10.1175/1520-0493(1998)126<0943:TIOMDO>2.0.CO;2).
- Graham, R. M., and Coauthors, 2019: Evaluation of six atmospheric reanalyses over Arctic sea ice from winter to early summer. *J. Climate*, **32**, 4121–4143, <https://doi.org/10.1175/JCLI-D-18-0643.1>.
- Grams, J. S., R. L. Thompson, D. V. Snively, J. A. Prentice, G. M. Hodges, and L. J. Reames, 2012: A climatology and comparison of parameters for significant tornado events in the United States. *Wea. Forecasting*, **27**, 106–123, <https://doi.org/10.1175/WAF-D-11-00008.1>.
- Groenemeijer, P., and T. Kühne, 2014: A Climatology of tornadoes in Europe: Results from the European Severe Weather Database. *Mon. Wea. Rev.*, **142**, 4775–4790, <https://doi.org/10.1175/MWR-D-14-00107.1>.
- , and Coauthors, 2017: Severe convective storms in Europe: Ten years of research and education at the European Severe Storms Laboratory. *Bull. Amer. Meteor. Soc.*, **98**, 2641–2651, <https://doi.org/10.1175/BAMS-D-16-0067.1>.
- Guastini, C. T., and L. F. Bosart, 2016: Analysis of a progressive derecho climatology and associated formation environments. *Mon. Wea. Rev.*, **144**, 1363–1382, <https://doi.org/10.1175/MWR-D-15-0256.1>.
- Hallgren, C., J. Arnoqvist, S. Ivanell, H. Körnich, V. Vakkari, and E. Sahlée, 2020: Looking for an offshore low-level jet champion among recent reanalyses: A tight race over the Baltic Sea. *Energies*, **13**, 3670, <https://doi.org/10.3390/en13143670>.
- Han, Y., Q. Yang, N. Liu, K. Zhang, C. Qing, X. Li, X. Wu, and T. Luo, 2021: Analysis of wind-speed profiles and optical turbulence above Gaomeigu and the Tibetan Plateau using ERA5 data. *Mon. Not. Roy. Astron. Soc.*, **501**, 4692–4702, <https://doi.org/10.1093/mnras/staa2960>.
- Hersbach, H., and Coauthors, 2020: The ERA5 global reanalysis. *Quart. J. Roy. Meteor. Soc.*, **146**, 1999–2049, <https://doi.org/10.1002/qj.3803>.
- Hipel, K. W., and A. I. McLeod, 1994: *Time Series Modelling of Water Resources and Environmental Systems*. Elsevier Science, 1013 pp.
- Hoogewind, K. A., M. E. Baldwin, and R. J. Trapp, 2017: The impact of climate change on hazardous convective weather in the United States: Insight from high-resolution dynamical downscaling. *J. Climate*, **30**, 10081–10100, <https://doi.org/10.1175/JCLI-D-16-0885.1>.
- Huang, J., J. Yin, M. Wang, Q. He, J. Guo, J. Zhang, X. Liang, and Y. Xie, 2021: Evaluation of five reanalysis products with radiosonde observations over the Central Taklimakan Desert during summer. *Earth Space Sci.*, **8**, e2021EA001707, <https://doi.org/10.1029/2021EA001707>.
- Ingrosso, R., P. Lionello, M. M. Miglietta, and G. Salvadori, 2020: A statistical investigation of mesoscale precursors of significant tornadoes: The Italian case study. *Atmosphere*, **11**, 301, <https://doi.org/10.3390/atmos11030301>.
- IPCC, 2014: *Climate Change 2014: Synthesis Report*. Cambridge University Press, 151 pp.
- Kattel, D. B., T. Yao, K. Yang, L. Tian, G. Yang, and D. Joswiak, 2012: Temperature lapse rate in complex mountain terrain on the southern slope of the central Himalayas. *Theor. Appl. Climatol.*, **113**, 671–682, <https://doi.org/10.1007/s00704-012-0816-6>.
- King, A. T., and A. D. Kennedy, 2019: North American supercell environments in atmospheric reanalyses and RUC-2. *J. Appl. Meteor. Climatol.*, **58**, 71–92, <https://doi.org/10.1175/JAMC-D-18-0015.1>.
- Koch, E., J. Koh, A. C. Davison, C. Lepore, and M. K. Tippett, 2021: Trends in the extremes of environments associated with severe U.S. thunderstorms. *J. Climate*, **34**, 1259–1272, <https://doi.org/10.1175/JCLI-D-19-0826.1>.
- Krocak, M. J., and H. E. Brooks, 2018: Climatological estimates of hourly tornado probability for the United States. *Wea. Forecasting*, **33**, 59–69, <https://doi.org/10.1175/WAF-D-17-0123.1>.

- Kunz, M., J. Sander, and C. Kottmeier, 2009: Recent trends of thunderstorm and hailstorm frequency and their relation to atmospheric characteristics in southwest Germany. *Int. J. Climatol.*, **29**, 2283–2297, <https://doi.org/10.1002/joc.1865>.
- Lepore, C., R. Abernathy, N. Henderson, J. T. Allen, and M. K. Tippett, 2021: Future global convective environments in CMIP6 models. *Earth's Future*, **9**, e2021EF002277, <https://doi.org/10.1029/2021EF002277>.
- Li, F., and D. R. Chavas, 2021: Midlatitude continental CAPE is predictable from large-scale environmental parameters. *Geophys. Res. Lett.*, **48**, e2020GL091799, <https://doi.org/10.1029/2020GL091799>.
- , —, K. A. Reed, and D. T. Dawson II, 2020: Climatology of severe local storm environments and synoptic-scale features over North America in ERA5 reanalysis and CAM6 simulation. *J. Climate*, **33**, 8339–8365, <https://doi.org/10.1175/JCLI-D-19-0986.1>.
- Liu, N., C. Liu, B. Chen, and E. Zipser, 2020: What are the favorable large-scale environments for the highest-flash-rate thunderstorms on Earth? *J. Atmos. Sci.*, **77**, 1583–1612, <https://doi.org/10.1175/JAS-D-19-0235.1>.
- Masroor, M., S. Rehman, R. Avtar, M. Sahana, R. Ahmed, and H. Sajjad, 2020: Exploring climate variability and its impact on drought occurrence: Evidence from Godavari Middle sub-basin, India. *Wea. Climate Extremes*, **30**, 100277, <https://doi.org/10.1016/j.wace.2020.100277>.
- McCarty, W., L. Coy, R. Gelaro, A. Huang, D. Merkova, E. B. Smith, M. Sienkiewicz, and K. Wargan, 2016: MERRA-2 input observations: Summary and initial assessment. NASA Tech. Rep. Series on Global Modeling and Data Assimilation Tech. Rep. NASA/TM-2016-104606, Vol. 46, 45 pp., <https://gmao.gsfc.nasa.gov/pubs/docs/McCarty885.pdf>.
- Minder, J. R., P. W. Mote, and J. D. Lundquist, 2010: Surface temperature lapse rates over complex terrain: Lessons from the Cascade Mountains. *J. Geophys. Res.*, **115**, D14122, <https://doi.org/10.1029/2009JD013493>.
- Mohr, S., and M. Kunz, 2013: Recent trends and variabilities of convective parameters relevant for hail events in Germany and Europe. *Atmos. Res.*, **123**, 211–228, <https://doi.org/10.1016/j.atmosres.2012.05.016>.
- , —, and B. Geyer, 2015: Hail potential in Europe based on a regional climate model hindcast. *Geophys. Res. Lett.*, **42**, 10904–10912, <https://doi.org/10.1002/2015GL067118>.
- , J. Wandel, S. Lenggenhager, and O. Martius, 2019: Relationship between atmospheric blocking and warm-season thunderstorms over western and central Europe. *Quart. J. Roy. Meteor. Soc.*, **145**, 3040–3056, <https://doi.org/10.1002/qj.3603>.
- Munich Re, 2020: Thunderstorms, hail and tornadoes: Localised but extremely destructive. Munich Re, accessed 29 November 2020, <https://www.munichre.com/en/risks/natural-disasters-losses-are-trending-upwards/thunderstorms-hail-and-tornados.html>.
- Pacey, G. P., D. M. Schultz, and L. Garcia-Carreras, 2021: Severe convective windstorms in Europe: Climatology, preconvective environments, and convective mode. *Wea. Forecasting*, **36**, 237–252, <https://doi.org/10.1175/WAF-D-20-0075.1>.
- Potvin, C. K., K. L. Elmore, and S. J. Weiss, 2010: Assessing the impacts of proximity sounding criteria on the climatology of significant tornado environments. *Wea. Forecasting*, **25**, 921–930, <https://doi.org/10.1175/2010WAF2222368.1>.
- Púčik, T., and Coauthors, 2017: Future changes in European severe convection environments in a regional climate model ensemble. *J. Climate*, **30**, 6771–6794, <https://doi.org/10.1175/JCLI-D-16-0777.1>.
- Rädler, A. T., P. Groenemeijer, E. Faust, and R. Sausen, 2018: Detecting severe weather trends using an Additive Regressive Convective Hazard Model (AR-CHaMo). *J. Appl. Meteor. Climatol.*, **57**, 569–587, <https://doi.org/10.1175/JAMC-D-17-0132.1>.
- , —, —, —, and T. Púčik, 2019: Frequency of severe thunderstorms across Europe expected to increase in the 21st century due to rising instability. *npj Climate Atmos. Sci.*, **2**, 30, <https://doi.org/10.1038/s41612-019-0083-7>.
- Rasmussen, E. N., and D. O. Blanchard, 1998: A baseline climatology of sounding-derived supercell and tornado forecast parameters. *Wea. Forecasting*, **13**, 1148–1164, [https://doi.org/10.1175/1520-0434\(1998\)013<1148:ABCOSD>2.0.CO;2](https://doi.org/10.1175/1520-0434(1998)013<1148:ABCOSD>2.0.CO;2).
- Rasmussen, K. L., A. F. Prein, R. M. Rasmussen, K. Ikeda, and C. Liu, 2020: Changes in the convective population and thermodynamic environments in convection-permitting regional climate simulations over the United States. *Climate Dyn.*, **55**, 383–408, <https://doi.org/10.1007/s00382-017-4000-7>.
- Riemann-Campe, K., K. Fraedrich, and F. Lunkeit, 2009: Global climatology of convective available potential energy (CAPE) and convective inhibition (CIN) in ERA-40 reanalysis. *Atmos. Res.*, **93**, 534–545, <https://doi.org/10.1016/j.atmosres.2008.09.037>.
- Rife, D. L., J. O. Pinto, A. J. Monaghan, C. A. Davis, and J. R. Hannan, 2010: Global distribution and characteristics of diurnally varying low-level jets. *J. Climate*, **23**, 5041–5064, <https://doi.org/10.1175/2010JCLI3514.1>.
- Robinson, E. D., R. J. Trapp, and M. E. Baldwin, 2013: The geospatial and temporal distributions of severe thunderstorms from high-resolution dynamical downscaling. *J. Appl. Meteor. Climatol.*, **52**, 2147–2161, <https://doi.org/10.1175/JAMC-D-12-0131.1>.
- Rodríguez, O., and J. Bech, 2020: Tornado environments in the Iberian Peninsula and the Balearic Islands based on ERA5 reanalysis. *Int. J. Climatol.*, **41**, E1959–E1979, <https://doi.org/10.1002/joc.6825>.
- Romps, D. M., A. B. Charn, R. H. Holzworth, W. E. Lawrence, J. Molinari, and D. Vollaro, 2018: CAPE times P explains lightning over land but not the land–ocean contrast. *Geophys. Res. Lett.*, **45**, 12623–12630, <https://doi.org/10.1029/2018GL080267>.
- Sander, J., J. F. Eichner, E. Faust, and M. Steuer, 2013: Rising variability in thunderstorm-related U.S. losses as a reflection of changes in large-scale thunderstorm forcing. *Wea. Climate Soc.*, **5**, 317–331, <https://doi.org/10.1175/WCAS-D-12-00023.1>.
- Sen, P. K., 1968: Estimates of the regression coefficient based on Kendall's tau. *J. Amer. Stat. Assoc.*, **63**, 1379–1389, <https://doi.org/10.1080/01621459.1968.10480934>.
- Shapiro, A., E. Fedorovich, and S. Rahimi, 2016: A unified theory for the Great Plains nocturnal low-level jet. *J. Atmos. Sci.*, **73**, 3037–3057, <https://doi.org/10.1175/JAS-D-15-0307.1>.
- Siedlecki, M., 2009: Selected instability indices in Europe. *Theor. Appl. Climatol.*, **96**, 85–94, <https://doi.org/10.1007/s00704-008-0034-4>.
- Smith, B. T., R. L. Thompson, J. S. Grams, C. Broyles, and H. E. Brooks, 2012: Convective modes for significant severe thunderstorms in the contiguous United States. Part I: Storm classification and climatology. *Wea. Forecasting*, **27**, 1114–1135, <https://doi.org/10.1175/WAF-D-11-00115.1>.

- Sulik, S., 2021: Formation factors of the most electrically active thunderstorm days over Poland (2002–2020). *Wea. Climate Extremes*, **34**, 100386, <https://doi.org/10.1016/j.wace.2021.100386>.
- Tang, B. H., V. A. Gensini, and C. R. Homeyer, 2019: Trends in United States large hail environments and observations. *npj Climate Atmos. Sci.*, **2**, 45, <https://doi.org/10.1038/s41612-019-0103-7>.
- Taszarek, M., H. E. Brooks, B. Czernecki, P. Szuster, and K. Fortuniak, 2018: Climatological aspects of convective parameters over Europe: A comparison of ERA-Interim and sounding data. *J. Climate*, **31**, 4281–4308, <https://doi.org/10.1175/JCLI-D-17-0596.1>.
- , P. Groenemeijer, J. T. Allen, R. Edwards, H. E. Brooks, V. Chmielewski, and S. E. Enno, 2020a: Severe convective storms across Europe and the United States. Part I: Climatology of lightning, large hail, severe wind, and tornadoes. *J. Climate*, **33**, 10239–10261, <https://doi.org/10.1175/JCLI-D-20-0345.1>.
- , J. T. Allen, T. Púčík, K. Hoogewind, and H. E. Brooks, 2020b: Severe convective storms across Europe and the United States. Part II: ERA5 environments associated with lightning, large hail, severe wind, and tornadoes. *J. Climate*, **33**, 10263–10286, <https://doi.org/10.1175/JCLI-D-20-0346.1>.
- , —, H. E. Brooks, N. Pilguy, and B. Czernecki, 2021a: Differing trends in United States and European severe thunderstorm environments in a warming climate. *Bull. Amer. Meteor. Soc.*, **102**, E296–E322, <https://doi.org/10.1175/BAMS-D-20-0004.1>.
- , N. Pilguy, J. T. Allen, V. A. Gensini, H. E. Brooks, and P. Szuster, 2021b: Comparison of convective parameters derived from ERA5 and MERRA-2 with rawinsonde data over Europe and North America. *J. Climate*, **34**, 3211–3237, <https://doi.org/10.1175/JCLI-D-20-0484.1>.
- Thompson, R. L., R. Edwards, J. A. Hart, K. L. Elmore, and P. Markowski, 2003: Close proximity soundings within supercell environments obtained from the Rapid Update Cycle. *Wea. Forecasting*, **18**, 1243–1261, [https://doi.org/10.1175/1520-0434\(2003\)018<1243:CPSWSE>2.0.CO;2](https://doi.org/10.1175/1520-0434(2003)018<1243:CPSWSE>2.0.CO;2).
- , B. T. Smith, J. S. Grams, A. R. Dean, and C. Broyles, 2012: Convective modes for significant severe thunderstorms in the contiguous United States. Part II: Supercell and QLCS tornado environments. *Wea. Forecasting*, **27**, 1136–1154, <https://doi.org/10.1175/WAF-D-11-00116.1>.
- Thorne, P. W., and R. S. Vose, 2010: Reanalyses suitable for characterizing long-term trends. *Bull. Amer. Meteor. Soc.*, **91**, 353–362, <https://doi.org/10.1175/2009BAMS2858.1>.
- Tippett, M. K., A. H. Sobel, S. J. Camargo, and J. T. Allen, 2014: An empirical relation between U.S. tornado activity and monthly environmental parameters. *J. Climate*, **27**, 2983–2999, <https://doi.org/10.1175/JCLI-D-13-00345.1>.
- , J. T. Allen, V. A. Gensini, and H. E. Brooks, 2015: Climate and hazardous convective weather. *Curr. Climate Change Rep.*, **1**, 60–73, <https://doi.org/10.1007/s40641-015-0006-6>.
- , C. Lepore, and J. E. Cohen, 2016: More tornadoes in the most extreme US tornado outbreaks. *Science*, **354**, 1419–1423, <https://doi.org/10.1126/science.aah7393>.
- , —, W. J. Koshak, T. Chronis, and B. Vant-Hull, 2019: Performance of a simple reanalysis proxy for U.S. cloud-to-ground lightning. *Int. J. Climatol.*, **39**, 3932–3946, <https://doi.org/10.1002/joc.6049>.
- Tochimoto, E., M. M. Miglietta, L. Bagagnoli, R. Inghrosso, and H. Niino, 2021: Characteristics of extratropical cyclones that cause tornadoes in Italy: A preliminary study. *Atmosphere*, **12**, 180, <https://doi.org/10.3390/atmos12020180>.
- Trapp, R. J., and K. A. Hoogewind, 2016: The realization of extreme tornadic storm events under future anthropogenic climate change. *J. Climate*, **29**, 5251–5265, <https://doi.org/10.1175/JCLI-D-15-0623.1>.
- Varga, Á. J., and H. Breuer, 2021: Evaluation of convective parameters derived from pressure level and native ERA5 data and different resolution WRF climate simulations over Central Europe. *Climate Dyn.*, <https://doi.org/10.1007/s00382-021-05979-3>, in press.
- Verbout, S. M., H. E. Brooks, L. M. Leslie, and D. M. Schultz, 2006: Evolution of the U.S. tornado database: 1954–2003. *Wea. Forecasting*, **21**, 86–93, <https://doi.org/10.1175/WAF910.1>.
- Vicente-Serrano, S. M., and Coauthors, 2018: Recent changes of relative humidity: Regional connections with land and ocean processes. *Earth Syst. Dyn.*, **9**, 915–937, <https://doi.org/10.5194/esd-9-915-2018>.
- Virman, M., M. Bister, J. Räisänen, V. A. Sinclair, and H. Järvinen, 2021: Radiosonde comparison of ERA5 and ERA-Interim reanalysis datasets over tropical oceans. *Tellus*, **73A** (1), 1–7, <https://doi.org/10.1080/16000870.2021.1929752>.
- Wang, Z., J. A. Franke, Z. Luo, and E. J. Moyer, 2021: Reanalyses and a high-resolution model fail to capture the “high tail” of CAPE distributions. *J. Climate*, **34**, 8699–8715, <https://doi.org/10.1175/JCLI-D-20-0278.1>.
- Westermayer, A., P. Groenemeijer, G. Pistotnik, R. Sausen, and E. Faust, 2017: Identification of favorable environments for thunderstorms in reanalysis data. *Meteor. Z.*, **26**, 59–70, <https://doi.org/10.1127/metz/2016/0754>.
- Wilcox, R. R., 2010: *Fundamentals of Modern Statistical Methods: Substantially Improving Power and Accuracy*. Springer, 249 pp.
- Wilson, J. W., and R. D. Roberts, 2006: Summary of convective storm initiation and evolution during IHOP: Observational and modeling perspective. *Mon. Wea. Rev.*, **134**, 23–47, <https://doi.org/10.1175/MWR3069.1>.
- Zhou, C., J. Wang, A. Dai, and P. Thorne, 2021: A new approach to homogenize global subdaily radiosonde temperature data from 1958 to 2018. *J. Climate*, **34**, 1163–1183, <https://doi.org/10.1175/JCLI-D-20-0352.1>.